
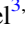







The Solar Neighborhood. XXXX. Parallax Results from the CTIOPI 0.9 m Program: New Young Stars Near the Sun

Jennifer L. Bartlett^{1,8} , John C. Lurie^{2,8} , Adric Riedel^{3,8} , Philip A. Ianna^{4,8}, Wei-Chun Jao^{5,8} , Todd J. Henry^{4,8}, Jennifer G. Winters^{6,8}, Charlie T. Finch^{1,8}, and John P. Subasavage^{7,8} 

¹ U.S. Naval Observatory, Washington, DC 20392, USA; jennifer.bartlett@navy.mil, charlie.finch@usno.navy.mil

² Department of Astronomy, University of Washington, Seattle, WA 98195, USA; lurie@uw.edu

³ California Institute of Technology, Pasadena, CA 91125, USA; adric.riedel@gmail.com

⁴ RECONS Institute, Chambersburg, PA 17201, USA; philianna3@gmail.com, thenry@chara.gsu.edu

⁵ Department of Physics and Astronomy, Georgia State University, Atlanta, GA 30302, USA; jao@chara.gsu.edu

⁶ Harvard-Smithsonian Center for Astrophysics, Cambridge, MA 02138, USA; jennifer.winters@cfa.harvard.edu

⁷ U.S. Naval Observatory, Flagstaff, AZ 86001, USA; jsubasavage@nobs.usno.navy.mil

Received 2016 June 21; revised 2017 August 1; accepted 2017 August 2; published 2017 September 15

Abstract

As a step toward completing and characterizing the census of the solar neighborhood, we present astrometric, photometric, and spectroscopic observations of 32 systems observed with the Cerro Tololo Inter-American Observatory 0.9 m and 1.5 m telescopes. Astrometry from the 0.9 m indicates that among the 17 systems that had no previous published trigonometric parallaxes, 14 are within 25 pc. In the full sample, nine systems have proper motions larger than $0''.5 \text{ yr}^{-1}$, including 2MASS J02511490-0352459, which exceeds $2''.0 \text{ yr}^{-1}$. *VRI* photometry from the 0.9 m and optical spectra from the 1.5 m indicate that the targets have $V = 11\text{--}22$ mag and spectral types M3.0V–L3.0V. For 2MASS J23062928-0502285 (TRAPPIST-1), we present updated astrometry and photometric variability based on over 12 years of observations. Of the nine binaries in the sample, two promise mass determinations in the next decade: LHS 6167AB, an M4.5V system for which we present an accurate parallax placing the binary at 9.7 pc, and 2MASS J23515048-2537367AB, an M8.5V system at 21.1 pc for which we present the first evidence of an unseen, low-mass companion. Most importantly, Na I and K I gravity indicators, H α measurements, long-term photometric variability, locations on the H-R diagram, and kinematic assessments indicate that as many as 13 of the systems are young, including candidate members of young moving groups, with ages less than ~ 120 Myr.

Key words: open clusters and associations: general – parallaxes – proper motions – solar neighborhood – stars: fundamental parameters – stars: late-type

1. Introduction

A well-understood, volume-limited sample of stellar systems is an essential input to determine the stellar luminosity and mass functions, the stellar velocity distribution, and the stellar multiplicity fraction. Although these physical relationships describe the makeup of our Galaxy, and by extension more distant galaxies, models are being developed from an incomplete catalog with limited parameters. Such volume-limited samples help define stellar populations and are critical to estimating the amount of mass contributed by local stars, while the systems in this volume provide insight into stellar evolution and the history of star formation in the Galactic disk. The nearby stars are also the brightest and easiest to examine in detail and allowing the detection of subtle differences among similar stars. These science topics have motivated the REsearch Consortium On Nearby Stars (RECONS⁹) to focus on

discovering and characterizing the nearest stars, with particular attention to those within 25 pc.

Trigonometric parallax (π_{trig}) is the only direct means of measuring stellar distances. Since 1999, the RECONS team has carried out the Cerro Tololo Inter-American Observatory (CTIO) Parallax Investigation (CTIOPI) at the 0.9 m and 1.5 m telescopes of the CTIO/Small and Moderate Aperture Research Telescope System (SMARTS). This ninth list of π_{trig} from CTIOPI presents astrometric, photometric, and spectroscopic observations of 32 southern systems with $V = 11\text{--}22$ mag and spectral types M3.0V–L3.0V.¹⁰ Earlier lists from CTIOPI highlighted systems with proper motions (μ) greater than $1''.0 \text{ yr}^{-1}$ (Jao et al. 2005) and between $0''.5$ and $1''.0 \text{ yr}^{-1}$ (Riedel et al. 2010), young stars (Riedel et al. 2014), subdwarfs (Jao et al. 2011), white dwarfs (Subasavage et al. 2009), and stars within 10 pc (Henry et al. 2006).

VRI photometry is collected to characterize the systems and to support parallax reductions. Aside from being an input to the parallax reduction pipeline, this homogeneous set of optical photometry supplements the infrared measurements available from the Two Micron All Sky Survey (Skrutskie et al. 2006, hereafter 2MASS; names are abbreviated to 2MASS HHMM-DDMM) for all of the systems. When combined with parallaxes, broadband colors such as these provide a rough

⁸ Visiting Astronomer, Cerro Tololo Inter-American Observatory. CTIO is operated by AURA, Inc. under contract to the National Science Foundation.

⁹ <http://www.recons.org>



Original content from this work may be used under the terms of the [Creative Commons Attribution 3.0 licence](https://creativecommons.org/licenses/by/3.0/). Any further distribution of this work must maintain attribution to the author(s) and the title of the work, journal citation and DOI.

¹⁰ As described in Section 5, the latest type object in the sample, 2MASS 0251-0352, likely is of type \sim L1V, making all 32 targets stars rather than brown dwarfs.

means of probing the temperatures, surface gravities, and compositions of nearby systems. In addition, photometric variability due to brief flares, rotation, or longer activity cycles can also provide insight into their stellar atmospheres.

Although spectroscopy is available in the literature for many nearby stars, RECONS spectroscopic observations provide spectral types and supply equivalent widths (EWs) of important lines and indices. The spectral type reflects the star’s surface temperature and gravity, from which its size and evolutionary stage can be estimated. The spectral line EWs and indices provide additional indications of youth and activity. The combination of parallaxes with this spectral information enables evaluations of stellar ages, while membership in a young moving group, or association, may be inferred based on astrometric assessments.¹¹ More precise age estimates for nearby stars increase their usefulness in understanding local star formation history, especially for the coolest and longest-lived stars.

The detection and characterization of multiple-star systems yields information about the star formation process, spanning systems with common proper motion and wide separations down to close systems for which stellar masses may soon be measured. In particular, newly identified close binaries can be resolved during astrometric or photometric observations or suggested by a perturbation in the astrometric residuals to a π_{trig} and μ solution.

In this paper, we provide π_{trig} , *VRI* photometry, optical spectroscopy, and information about multiplicity for the 32 systems targeted. The results presented here supersede those reported earlier (Bartlett 2007a, 2007b; Bartlett et al. 2007), owing to additional observations and improved reduction techniques (Subasavage et al. 2009). In addition, Bartlett et al. (2016a, 2016b, 2017) partially characterized some systems based on this study.

2. Observations and Data Reduction

Southern systems without π_{trig} that were identified to be possibly within 25 pc via photometric or spectroscopic distance estimates were culled from the literature available in 2003 October. To ensure the candidates were bright enough to be observed by the 0.9 m telescope with exposure times no longer than ~ 1200 s, magnitude limits of $V = 15$, $I = 16$, or $J = 13.1$ were imposed insofar as published photometry was available in these bands; in a few cases, our subsequent photometry determined that a target was fainter than initially thought. A total of 43 candidate systems were identified for π_{trig} measurements, which was reduced to the 32 targets for which we provide astrometric, photometric, and spectroscopic results here.

2.1. Astrometry

The CTIO/SMARTS 0.9 m telescope has a 2048×2048 Tektronix CCD camera with $0''.401 \text{ pixel}^{-1}$ plate scale (Jao et al. 2003). The center quarter of the chip with a $6''.8$ square field of view is used for both astrometric and photometric observations during CTIOPI. An optimal filter is selected for each π_{trig} target and set of reference stars in one of three bandpasses: “old” V_J and/or “new” V_J , R_{KC} or I_{KC} ¹² (hereafter

¹¹ Obtaining radial velocities would enable stellar motions to be characterized more fully, but the resolution obtained with the CTIO/SMARTS 1.5 m observations described here is insufficient for such measurements.

¹² The central wavelengths for the “old” V_J , “new” V_J , R_{KC} , and I_{KC} filters are 5438, 5475, 6425, and 8075 Å, respectively.

without the subscripts). Throughout the course of the observations, the field of target and reference stars, which ideally encircle the target, is positioned to within a few pixels. Exposure times varied from 20 to 1200 s to accommodate the brightnesses of the science targets and reference stars and to adjust for sky conditions. For best centroiding, the measured stars have maximum peak counts of $\sim 50,000$, which is less than the saturation value of 65,535 counts. Typically, 3–10 frames are taken per night within ± 30 minutes of the transit time of the field to minimize corrections for differential color refraction (DCR). Nightly collection of bias and dome flat frames supports the routine calibration of the science images.

Two *V* filters were used during the 12 years of observations described here: the “old” Tektronix#2 *V* filter and the “new” Tektronix#1 *V* filter. The old *V* filter cracked in 2005 February and was replaced with the new *V* filter, which was used between 2005 and 2009. After determining that the crack in its corner did not affect astrometric residuals significantly, the old *V* filter was returned to service in 2009 July. Subasavage et al. (2009) ascertained that combined data from these filters can produce a reliable π_{trig} as long as at least 1–2 years of data, depending on observational frequency, were collected in each. In total, 11 of the 32 systems in this sample were observed astrometrically in the *V* band; the reductions of two systems used frames from the old filter exclusively, eight used frames from both, and one used frames from the new filter only. Subasavage et al. (2009) and Riedel et al. (2010) discuss the two filters and their astrometric performance in greater detail.

Jao et al. (2005) and Henry et al. (2006) describe the CTIOPI data reduction processes. To summarize, centroids for the measured stars are obtained using SExtractor (Bertin & Arnouts 1996, hereafter SExtractor)¹³ and corrected for DCR using *VRI* photometry for the target and reference stars. The relative π_{trig} and μ of the science star are obtained using the GaussFit program (Jefferys et al. 1987, hereafter GaussFit)¹⁴ using a six-constant plate model and assuming that the selected reference stars have zero mean π_{trig} and μ . A correction from relative to absolute π_{trig} is obtained using the weighted mean distance to the set of reference stars. For each reference star, a photometric distance is estimated through comparison of its *VRI* colors to the colors and absolute *V*-band magnitudes (M_V) of single, main-sequence stars in the 10 pc sample (Henry et al. 2006).

2.2. Photometry

To obtain *VRI* photometry of the targets and reference stars, the CTIO/SMARTS 0.9 m telescope was used in the same configuration as described above for astrometry, including nightly bias and dome flat frames. Fields were typically observed at air masses $\text{sec } z \leq 1.4$. Exposure times varied in order to reach a signal-to-noise ratio greater than 100 for each π_{trig} candidate in all three bands. During each night, additional fields of standard stars from Graham (1982), Bessel (1990), and Landolt (1992, 2007, 2013) were observed several times to derive transformation equations and extinction curves. Photometric reductions used an aperture of $7''$ radius around the star of interest, similar to that used by Landolt (1992); if the

¹³ Available from the Institut d’Astrophysique de Paris (IAP) at <http://www.astromatic.net/software/sextractor>.

¹⁴ Available from the Hubble Space Telescope (HST) Astrometry Team at <ftp://clyde.as.utexas.edu/pub/gaussfit/>.

standard aperture included a contaminating source, then an aperture correction was made. Jao et al. (2005) and Winters et al. (2011) discuss the photometric data reductions, definition of transformation equations, and errors in greater detail.

The V measurements for 13 systems in this sample combine values from the two different V filters discussed in Section 2.1; the remaining V measurements combine data from nights using a single filter. Jao et al. (2011) evaluated 10 photometric standard stars observed in both filters and concluded that photometry from the two filters can be combined without adding significant systematic errors.

2.3. Photometric Variability

The long-term observations of these fields (up to 12 years) were analyzed to assess the photometric variability of the π_{trig} targets. Because photometric standard stars were not observed on every night during which astrometric observations were collected, the relative fluxes of the targets were compared to their reference stars to obtain corrected instrumental magnitudes instead of apparent magnitudes, using SExtractor with apertures of 6" diameter. We use the prescription of Honeycutt (1992) to handle the inhomogeneous sets of exposures, resulting in instrumental magnitudes for target and reference stars in each frame that include varying effects of sky conditions, extinction, and exposure times. GaussFit was then used to obtain instrumental magnitude offsets for the images, from which corrected magnitudes could be calculated. The standard deviations of the corrected magnitudes for each star of interest were evaluated, and any outlying reference stars removed from the calculation; corrected magnitudes were then recalculated, if necessary. The standard deviation of final corrected magnitudes for a π_{trig} target indicates its intrinsic variability around its mean magnitude. However, a flare occurring on a single night during a series of observations could also produce a high standard deviation. Jao et al. (2011) and Hosey et al. (2015) discuss the RECONS method of variability analysis in greater detail.

2.4. Spectroscopy

The Ritchey–Chrétien spectrograph with a 2" slit and Loral 1200 × 800 CCD camera were used on the CTIO/SMARTS 1.5 m telescope to obtain optical spectroscopy for the sample. Spectra covering the range 6000–9500 Å with a resolution of 8.6 Å were obtained using grating #32 in first order at a tilt of 15°.1 and order-blocking filter OG570. To reject cosmic rays, at least two exposures were taken for each object; additional exposures were taken for the faintest system.

At the beginning of each night, bias frames, dome flats, and sky flats were taken for calibration. For wavelength calibration, a 10 s spectrum of either a neon–helium–argon (Ne+He+Ar) or a neon-only arc lamp was recorded after each science observation. In addition, spectroscopic flux standard stars found in the Image Reduction and Analysis Facility (Tody 1986, 1993, hereafter IRAF)¹⁵ spectroscopy reduction packages were observed at least once during each observing run, and usually nightly. Because the initial intention was to obtain spectral types only, no telluric standards were observed.

Reductions were processed using the appropriate IRAF packages, in particular *onedspec.dispcor* for wavelength calibrations and *onedspec.calibrate* for flux calibrations.

Assignment of spectral types followed the method of Jao et al. (2008) and Riedel et al. (2014) using the same set of spectral standard dwarfs. Spectral line EWs and indices were computed utilizing 11 Å windows centered on the maximum or minimum of the feature for both the H α line at 6563 Å and the neutral potassium (K I) doublet at 7699 Å. Full bins of 24 Å were used for the neutral sodium (Na I) doublet at 8184 and 8195 Å. The Na I doublet and the 7665 Å line of the K I doublet are in uncorrected telluric absorption bands, the depths of which can be significant at the CTIO altitude of ~2200 m. This possible contamination contributes to the large uncertainties in the values obtained. The 7699 Å line in the K I doublet should be just outside the telluric absorption band with less than 4% contamination (Hinkle et al. 2003). Finally, with a resolving power less than 1500, the RECONS spectra are insufficient for measuring accurate radial velocities.

3. Results

A target is typically observed until the π_{trig} error is less than 3 mas based on at least 40 frames collected over at least two years. In addition, at least two nights of VRI photometry, and preferably three, are typically acquired. Results for the 32 targets described here meet these criteria in nearly every case.

3.1. Astrometry

The astrometry for all 32 systems measured appears in Table 1. The first three columns describe the systems by name and position. Columns 4–9 provide the observational details: filter used, number of seasons observed, number of frames used in reductions, dates of observations, time span, and number of reference stars. The relative π_{trig} , parallax correction, absolute π_{trig} , μ , position angle (P.A.) of μ , and the derived tangential velocity appear in columns 10–15. The positions in columns 2 and 3 are based on 2MASS positions adjusted to epoch 2000.0 using the relative μ and position angles listed in columns 13 and 14. The tangential velocities in column 15 are computed from the relative μ and absolute π_{trig} . Section 5 discusses in greater detail the individual systems marked with an exclamation mark (“!”) in the notes column.

The measured distances range from 7.6 pc for Fomalhaut C to 36.0 pc for LP 822-101, including 14 new systems within 25 pc. In addition to Fomalhaut C, which we reported to be within 10 pc for the first time in Mamajek et al. (2013), we provide an accurate π_{trig} for LHS 6167AB that places it within 10 pc. We find that three systems, LHS 2880, LP 932-83, and LP 822-101, which were previously considered to lie within 25 pc based on less accurate photometric estimates, are actually 30–36 pc away.

Systems with high proper motion are likely candidates for being nearby stars, because the annual change is inversely proportional to stellar distance. All but three systems in this sample have μ greater than 0".2 yr⁻¹, with nine exceeding 0".5 yr⁻¹. The corresponding tangential velocities range from 10.4 to 112.4 km s⁻¹, with a median value of 27.1 km s⁻¹.

The final absolute π_{trig} errors for this sample are 0.6–3.0 mas. The single-measurement accuracy for well-balanced reference fields with exposures at least a few minutes in duration is typically 2–4 mas; however, errors may be as high as 20 mas

¹⁵ IRAF is distributed by the National Optical Astronomy Observatories (NOAO), which are operated by the Association of Universities for Research in Astronomy, Inc. (AURA), under cooperative agreement with the National Science Foundation (NSF); it is available at <http://iraf.noao.edu/>.

Table 1
Astrometric Results

System Name (1)	R.A. (J2000.0) (2)	Decl. (J2000.0) (3)	Fil. (4)	N_{lea} (5)	N_{frm} (6)	Coverage (7)	Years (8)	N_{ref} (9)	$\pi(\text{rel})$ (mas) (10)	$\pi(\text{corr})$ (mas) (11)	$\pi(\text{abs})$ (mas) (12)	μ (mas yr $^{-1}$) (13)	P.A. (deg) (14)	V_{tan} (km s $^{-1}$) (15)	Notes (16)
LP 991-84	01 39 21.72	-39 36 09.1	<i>V</i>	6s	66	2003.94-2012.96	9.02	8	115.21 \pm 1.33	0.69 \pm 0.09	115.90 \pm 1.33	258.9 \pm 0.4	146.7 \pm 0.19	10.6	^a , !
LHS 1363	02 14 12.56	-03 57 43.6	<i>I</i>	10s	64	2003.94-2012.95	9.01	7	80.40 \pm 1.12	1.73 \pm 0.20	82.13 \pm 1.14	532.5 \pm 0.4	107.0 \pm 0.07	30.7	
G75-35	02 41 15.14	-04 32 17.8	<i>R</i>	9s	73	2003.95-2012.94	8.99	9	83.87 \pm 1.38	0.84 \pm 0.05	84.71 \pm 1.38	357.5 \pm 0.5	97.4 \pm 0.12	20.0	^b , !
2MASS 0251-0352	02 51 15.00	-03 52 48.1	<i>I</i>	9s	53	2003.95-2012.94	8.99	8	89.95 \pm 3.02	0.67 \pm 0.07	90.62 \pm 3.02	2149.7 \pm 0.9	149.2 \pm 0.05	112.4	!
LP 888-18	03 31 30.25	-30 42 38.8	<i>I</i>	9s	69	2003.95-2012.88	8.93	7	79.63 \pm 1.07	0.69 \pm 0.04	80.32 \pm 1.07	408.8 \pm 0.3	172.3 \pm 0.08	24.1	^c , !
LP 889-37	04 08 55.58	-31 28 54.0	<i>R</i>	8s	63	2003.95-2012.94	8.99	7	63.77 \pm 1.75	0.58 \pm 0.06	64.35 \pm 1.75	255.2 \pm 0.7	181.6 \pm 0.22	18.8	
LHS 5094	04 26 32.65	-30 48 01.9	<i>V</i>	10s	66	2003.95-2012.95	9.00	7	75.03 \pm 2.90	0.36 \pm 0.13	75.39 \pm 2.90	478.4 \pm 1.0	189.0 \pm 0.19	30.1	
2MASS 0429-3123AB	04 29 18.43	-31 23 56.7	<i>R</i>	8s	69	2003.95-2012.95	8.99	13	57.99 \pm 1.25	0.72 \pm 0.08	58.71 \pm 1.25	129.4 \pm 0.5	38.9 \pm 0.40	10.4	!
LP 834-32	04 35 36.19	-25 27 34.9	<i>V</i>	8s	64	2003.95-2011.74	7.79	11	56.56 \pm 1.78	1.08 \pm 0.10	57.64 \pm 1.78	202.1 \pm 0.7	162.4 \pm 0.37	16.6	!
LP 776-25	04 52 24.42	-16 49 22.2	<i>V</i>	3c	47	2005.89-2008.12	2.24	7	68.33 \pm 1.70	1.07 \pm 0.09	69.40 \pm 1.70	245.0 \pm 2.2	151.3 \pm 1.00	16.7	^d , !
2MASS 0517-3349	05 17 37.70	-33 49 03.1	<i>I</i>	9s	64	2003.95-2012.94	8.99	10	60.25 \pm 1.53	1.32 \pm 0.21	61.57 \pm 1.54	548.8 \pm 0.6	126.8 \pm 0.12	42.2	
LP 717-36AB	05 25 41.67	-09 09 12.6	<i>V</i>	6s	55	2003.96-2010.17	6.21	7	46.72 \pm 1.37	2.35 \pm 0.30	49.07 \pm 1.40	200.0 \pm 0.8	167.7 \pm 0.39	19.3	^e , !
LHS 6167AB	09 15 36.40	-10 35 47.2	<i>V</i>	10s	113	2003.94-2013.25	9.31	8	102.25 \pm 0.98	1.08 \pm 0.18	103.33 \pm 1.00	439.4 \pm 0.3	244.6 \pm 0.07	20.2	^f , !
2MASS 0921-2104	09 21 14.10	-21 04 44.4	<i>I</i>	10s	66	2004.18-2013.12	8.94	11	80.53 \pm 1.04	0.55 \pm 0.05	81.08 \pm 1.04	948.9 \pm 0.3	164.7 \pm 0.04	55.5	
G161-71	09 44 54.18	-12 20 54.4	<i>V</i>	9s	80	2003.94-2012.96	9.02	8	72.87 \pm 1.42	1.23 \pm 0.16	74.10 \pm 1.43	321.1 \pm 0.6	277.1 \pm 0.16	20.5	^g , !
LP 731-76	10 58 27.99	-10 46 30.5	<i>I</i>	8s	167	2004.43-2011.50	7.07	5	70.33 \pm 1.51	2.89 \pm 0.76	73.22 \pm 1.69	212.3 \pm 0.8	248.0 \pm 0.37	13.7	!
LHS 2783AB	13 42 09.97	-16 00 23.4	<i>R</i>	7c	105	2005.09-2011.42	6.32	7	50.83 \pm 0.92	3.04 \pm 0.67	53.87 \pm 1.14	503.6 \pm 0.4	267.1 \pm 0.08	44.3	!
LP 739-2	13 58 16.18	-12 02 59.1	<i>I</i>	6c	70	2005.10-2010.16	5.06	6	53.11 \pm 1.33	1.13 \pm 0.09	54.24 \pm 1.33	340.3 \pm 1.0	277.5 \pm 0.26	29.7	!
LHS 2880	14 13 04.86	-12 01 26.8	<i>R</i>	6s	82	2004.58-2009.49	4.91	8	30.88 \pm 1.35	1.45 \pm 0.13	32.33 \pm 1.36	711.3 \pm 0.9	237.0 \pm 0.15	104.3	!
2MASS 1507-2000	15 07 27.81	-20 00 43.3	<i>I</i>	7s	74	2004.45-2011.16	6.71	6	41.64 \pm 0.62	0.89 \pm 0.12	42.53 \pm 0.63	129.1 \pm 0.5	121.9 \pm 0.40	14.4	!
LHS 3056	15 19 11.74	-12 45 06.7	<i>V</i>	4s	44	2004.58-2007.43	2.85	8	46.71 \pm 2.08	0.54 \pm 0.10	47.25 \pm 2.08	759.9 \pm 2.5	256.7 \pm 0.32	76.2	^h , !
2MASS 1534-1418	15 34 56.93	-14 18 49.2	<i>I</i>	7s	62	2004.60-2012.17	7.57	6	90.60 \pm 0.82	0.91 \pm 0.04	91.51 \pm 0.82	972.6 \pm 0.4	251.5 \pm 0.05	50.4	ⁱ
LP 869-19AB	19 42 00.66	-21 04 05.6	<i>R</i>	6c	63	2004.57-2009.31	4.74	13	51.58 \pm 1.58	2.23 \pm 0.17	53.81 \pm 1.59	257.0 \pm 0.9	163.9 \pm 0.34	22.6	^j , !
LP 869-26AB	19 44 53.80	-23 37 59.4	<i>R</i>	5c	55	2004.57-2008.71	4.14	9	66.24 \pm 1.10	1.63 \pm 0.08	67.87 \pm 1.10	348.7 \pm 0.7	117.7 \pm 0.21	24.4	!
LP 870-65	20 04 30.79	-23 42 02.4	<i>R</i>	7s	68	2004.57-2010.50	5.92	6	53.79 \pm 1.59	1.21 \pm 0.15	55.00 \pm 1.60	357.0 \pm 0.8	160.9 \pm 0.23	30.8	^k , !
LP 756-3	20 46 43.64	-11 48 13.3	<i>R</i>	7s	68	2004.58-2010.73	6.15	12	50.99 \pm 1.36	1.43 \pm 0.22	52.42 \pm 1.38	352.0 \pm 0.6	100.4 \pm 0.16	31.8	^l , !
LP 984-92	22 45 00.07	-33 15 26.0	<i>R</i>	7s	58	2004.58-2011.62	7.03	7	46.76 \pm 2.34	1.08 \pm 0.14	47.84 \pm 2.34	215.0 \pm 0.9	122.9 \pm 0.49	21.3	^m , !
Fomalhaut C	22 48 04.50	-24 22 07.8	<i>V</i>	8s	118	2004.44-2012.88	8.44	6	131.14 \pm 1.16	0.93 \pm 0.25	132.07 \pm 1.19	378.1 \pm 0.4	118.0 \pm 0.12	13.6	ⁿ , !
LP 932-83	22 49 08.41	-28 51 20.1	<i>V</i>	6s	47	2004.58-2011.50	6.92	8	29.38 \pm 2.09	0.41 \pm 0.05	29.79 \pm 2.09	296.2 \pm 0.9	218.4 \pm 0.33	47.1	!

Table 1
(Continued)

System Name	R.A. (J2000.0) (2)	Decl. (J2000.0) (3)	Fil. (4)	N_{sea} (5)	N_{frm} (6)	Coverage (7)	Years (8)	N_{ref} (9)	$\pi(\text{rel})$ (mas) (10)	$\pi(\text{corr})$ (mas) (11)	$\pi(\text{abs})$ (mas) (12)	μ (mas yr ⁻¹) (13)	P.A. (deg) (14)	V_{tan} (km s ⁻¹) (15)	Notes (16)
2MASS 2306-0502	23 06 29.36	-05 02 29.2	<i>I</i>	10s	72	2004.58-2016.73	12.15	7	78.14 ± 1.04	0.62 ± 0.06	78.76 ± 1.04	1034.8 ± 0.3	118.5 ± 0.03	62.3	°
LP 822-101	23 31 25.04	-16 15 57.8	<i>V</i>	6s	58	2004.60-2011.62	7.01	6	26.96 ± 1.96	0.81 ± 0.07	27.77 ± 1.96	346.4 ± 1.1	137.5 ± 0.37	59.1	!
2MASS 2351- 2537AB	23 51 50.48	-25 37 36.7	<i>I</i>	6c	65	2004.58-2012.88	8.30	9	46.76 ± 1.03	0.49 ± 0.04	47.25 ± 1.03	400.0 ± 0.4	61.9 ± 0.10	40.1	!

Notes. N_{sea} indicates the number of seasons observed, where 3–6 months of observations count as one season for seasons in which more than three images were taken. A “c” indicates a continuous set of observations with multiple nights of data collected in each season while an “s” indicates scattered observations because at least one season has only one night of observations. Generally, “c” observations are better than “s.” Systems with exclamation marks in the Notes column are discussed in Section 5.

^a Parallax in Weinberger et al. (2016) = 113.69 ± 0.54 mas.

^b Parallax in Finch & Zacharias (2016) = 90.0 ± 9.5 mas.

^c Parallax in Weinberger et al. (2016) = 78.99 ± 1.10 mas.

^d Parallaxes in Shkolnik et al. (2012) = 61.4 ± 1.5 mas and *Gaia* = 63.40 ± 0.36 mas.

^e Parallax in Shkolnik et al. (2012) = 48.2 ± 5.0 mas.

^f Parallax in Finch & Zacharias (2016) = 134.9 ± 12.1 mas.

^g Parallaxes in Weinberger et al. (2016) = 75.39 ± 0.85 mas and Finch & Zacharias (2016) = 96.1 ± 15.9 mas.

^h Parallaxes in Weinberger et al. (2016) = 47.34 ± 3.67 mas and Finch & Zacharias (2016) = 43.3 ± 16.9 mas.

ⁱ Parallax in Weinberger et al. (2016) = 91.23 ± 0.63 mas.

^j Parallax in Weinberger et al. (2016) = 53.68 ± 0.64 mas.

^k Parallax in Weinberger et al. (2016) = 54.89 ± 0.57 mas.

^l Parallax in Shkolnik et al. (2012) = 53.5 ± 1.3 mas.

^m Parallax in Shkolnik et al. (2012) = 45.5 ± 3 mas.

ⁿ Parallax in Weinberger et al. (2016) = 129.57 ± 0.31 mas. The CTIOPI parallax listed here is identical to our value in Mamajek et al. (2013).

^o Parallaxes in Costa et al. (2006) = 82.58 ± 2.58 and Weinberger et al. (2016) = 80.09 ± 1.17 mas. Also known as TRAPPIST-1.

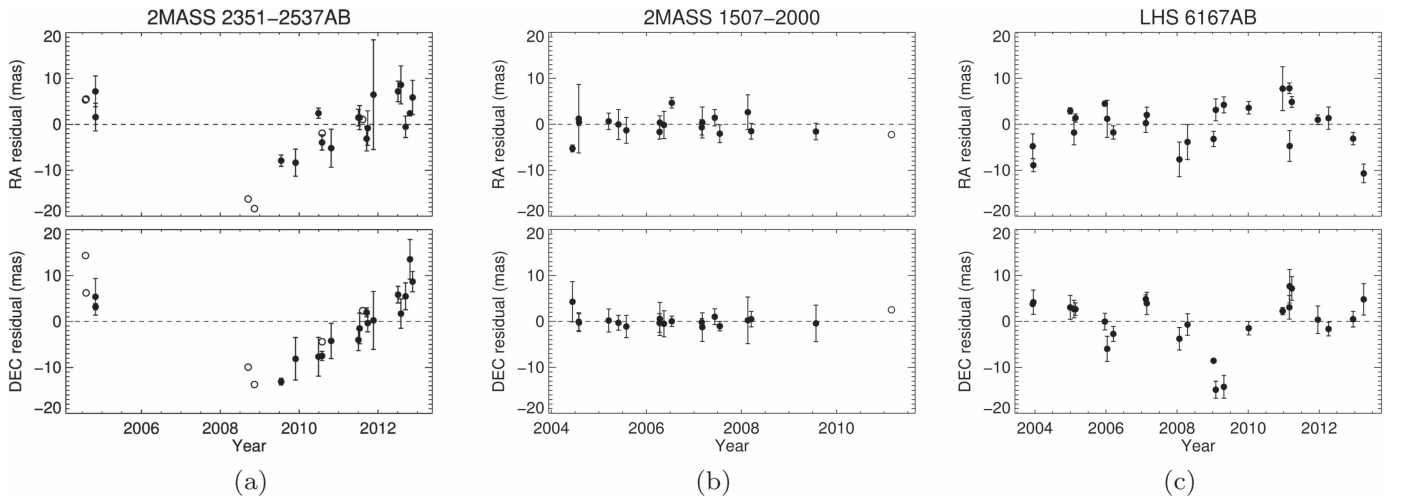


Figure 1. Nightly mean astrometric residuals in R.A. and decl. are shown for 2MASS J23515044-2537367AB (perturbation), 2MASS J15072779-2000431 (no detected perturbation), and LHS 6167AB (possible perturbation). The astrometric signatures of each system’s μ and π_{trig} have been removed. Filled circles represent nightly means while open circles represent nights from which only one frame is available.

Table 2
Comparison of Proper Motions for 2MASS J02511490-0352459

Technique (1)	μ (mas yr ⁻¹) (2)	P.A. (deg) (3)	V_{tan} (km s ⁻¹) (4)	References (5)
CTIOPI astrometry	2150 ± 1	149.2 ± 0.1	112.4 ± 3.4	1
SuperCOSMOS-2MASS	2185 ± 57	149.3	...	2
DSS-2MASS	2170 ± 110	149.0 ± 2.0	124.6 ± 13.1	3
2MASS-UKIRT	2140 ± 20	148 ± 0.6	122 ± 11	4

Note. (1) This work, (2) Deacon et al. (2005), (3) Schmidt et al. (2007), (4) Jameson et al. (2008) and Faherty et al. (2009).

for poor reference fields, shorter exposure times, and binaries with asymmetric point-spread functions. Weak reference fields contain fewer than five reference stars, have lopsided configurations, or have very faint reference stars. The quality of a particular solution may be assessed by evaluating the nightly residuals in each axis; for instance, Figure 1(b) shows a good solution with nearly flat residuals for 2MASS 1507-2000 after the removal of the astrometric signatures of its μ and π_{trig} . For comparison, Figure 1(a) shows a perturbation in the residuals of 2MASS 2351-2537AB while Figure 1(c) may display a perturbation in the residuals of LHS 6167AB.

3.1.1. Comparison to Other Parallax Results

Several other programs have measured π_{trig} for some of the systems in this sample: the CTIOPI 1.5 m program (Costa et al. 2005), the Carnegie Astrometric Planet Search (Boss et al. 2009; Shkolnik et al. 2012; Weinberger et al. 2016), the United States Naval Observatory (USNO) Robotic Astrometric Telescope (URAT) program (Finch & Zacharias 2016), and *Gaia* (Gaia Collaboration et al. 2016a, 2016b; Lindgren et al. 2016). Additional π_{trig} for 15 of the targets in the program discussed here are given in the notes to Table 1. As found in previous papers in this series, the agreement between CTIOPI π_{trig} and other programs is excellent with no systematic offsets.

Bartlett (2007a) presented preliminary astrometry from this program for all of these systems except 2MASS 2351-2537AB. The final values herein are consistent with those earlier results. In addition, Mamajek et al. (2013) reported a π_{trig} for

Fomalhaut C based on the CTIOPI astrometry presented herein; we list the same result here to complete the sample of 32 targets on the program.

3.1.2. Comparison to Other Tangential Velocities

The median tangential velocity of 27.1 km s⁻¹ for this sample is consistent with the median of 28.6 km s⁻¹ found by Winters et al. (2017) for a sample of 151 M dwarf systems. In addition, Faherty et al. (2009) and Zapatero Osorio et al. (2007) obtained mean tangential velocities for samples of red and brown dwarfs within 20 pc and found similar distributions. Therefore, the median tangential velocity of our sample appears consistent with other samples we have observed at the CTIOPI/SMARTS 0.9 m and other studies of the field population of M dwarfs, although other age metrics suggest that some systems may be young or old, as discussed in Sections 3.4 and 4.2.

The single standout in our sample is 2MASS 0251-0352, with $V_{\text{tan}} = 112.4$ km s⁻¹; at just over 2'' yr⁻¹, it has the largest μ in the sample. Deacon et al. (2005), Schmidt et al. (2007), and Jameson et al. (2008) measured similarly large μ for 2MASS 0251-0352 by comparing the 2MASS position of this system with its SuperCOSMOS, Digitized Sky Survey (DSS), and 2006 United Kingdom Infrared Telescope (UKIRT) positions, respectively. These measurements are collected in Table 2. Although the CTIOPI position angle is almost 1% greater than that measured by Jameson et al. (2008), all the other values agree within the reported errors. Jameson et al. (2008) identify 2MASS 0251-0352 kinematically as a member of the thick disk of the Galaxy with an approximate age of

10 Gyr; Faherty et al. (2009) similarly place this system in a distinct high-velocity population that is probably older than most late M and L dwarfs in the solar neighborhood.

3.2. *VRI* Photometry

When observations began, no *V*-band photometry was available for 11 systems in this sample. Now, *VRI* photometry is given for all of the targets in Table 3, supplemented with the near-infrared photometry (*J*, *H*, and *K_s* bands) from 2MASS. Names and positions are given in the first three columns, followed by the optical *VRI* photometry, the number of nights of *VRI* observations, and the reference in columns 4–8. Photometric variability results (see Section 3.3) are listed in columns 9–12. The 2MASS *JHK_s* photometry is given in columns 13–15. For binaries that were unresolved by the CTIOPI/SMARTS 0.9 m (astrometry, photometry) and 1.5 m (spectroscopy) telescopes, joint photometry is given, identified by “J” in column 18.

As discussed in detail in Winters et al. (2011), errors in the *VRI* photometry program are typically ≤ 0.03 mag. However, systems that are faint in *V* sometimes have larger errors, e.g., the faintest system, 2MASS 0251-0352, has $V = 21.61 \pm 0.24$ mag. All other systems in the sample discussed here have errors less than 0.07 mag in *V*.

3.3. Photometric Variability

Column 10 of Table 3 lists the variability of each target in the filter used for astrometric observations, measured using the standard deviations in millimagnitudes. The systems in this sample range in variability from 8 to 46 mmag. Jao et al. (2011) and Hosey et al. (2015) established a floor of 7 mmag, below which variability cannot be detected by CTIOPI observations and this type of analysis, and set 20 mmag as the minimum standard deviation for a system to be considered significantly variable. Seven systems (22%) demonstrate significant variability: LHS 5094, LP 834-32, G161-71, LP 932-83, and LHS 6167AB in *V*; LP 984-92 in *R*; and LP 731-76 in *I*. Figure 2(a) shows the light curve of LP 731-76 around its mean magnitude, including a flare in 2006 and an overall variability of 35 mmag in the *I* band. LP 834-32, LHS 6167AB, LP 932-83, and 2MASS 2306-0502 also show evidence of flaring during the course of observations, as indicated in column 12. For comparison, the light curve of the least variable star in the sample, 2MASS 1534-1418 with an *I*-band variability measurement of only 8 mmag, is shown in Figure 2(b).

Weis (1994) and Jao et al. (2011) found that red dwarfs are more variable in the *V* and *R* bands than in the *I* band. Hosey et al. (2015) confirmed this and quantified the fractions of 238 red dwarfs within 25 pc that were variable by 20 mmag, finding 13% in *V*, 4% in *R*, and 3% in *I*. Of the seven systems varying by at least 20 mmag in the sample discussed here, 5/11 (45%) were observed in *V*, 1/10 (10%) was observed in *R*, and 1/11 (9%) was observed in *I*, showing the same general trend as found in Hosey et al. (2015). While flares in M dwarfs are bright in continuum emission at shorter wavelengths (Hawley & Petterson 1991), only 3/7 (43%) systems in this sample with significant variability also appeared to undergo a flare.

Mamajek et al. (2013) estimated the intrinsic variability of Fomalhaut C to be ~ 50 mmag in *V* based on published photometry plus our measurements. However, analysis of the consistent, long-term data from CTIOPI indicates that its

V-band variability is about only 12 mmag, or essentially quiescent.

3.4. Spectroscopy

Column 16 of Table 3 reports RECONS spectral types for 25 M dwarfs in this sample and literature values for the remaining seven, including two early L dwarfs. Types for systems with combined spectra of two components are listed with “J” in column 18. The RECONS spectral types reported here range from M3.0V to M8.5V with an uncertainty in classification of ± 0.5 subtype. G75-35 (M4.0V), LP 776-25 (M3.0V), and Fomalhaut C (M4.0V) are among the M dwarf standards used in determining spectral types. With one exception, the RECONS types agree, within the associated errors, with those available in the literature and the preliminary values from this program (Bartlett 2007a). For 2MASS 0429-3123AB, the RECONS type of M5.5V differs by more than a subtype from the previously reported value of M7.5V (Cruz et al. 2003); neither group resolved this system in their spectra.

Spectra from the CTIO/SMARTS 1.5 m telescope are also used to measure three signatures of youth and activity (Riedel et al. 2014): the $H\alpha$ line at 6563 Å, the Na I doublet at 8184 and 8195 Å, and half of the K I doublet at 7699 Å. Columns 3–6 of Table 4 present the $H\alpha$, Na I, and K I measurements for most systems in this sample. The Na I measurement is expressed using the gravity index from Lyo et al. (2004) and as an EW. The Na I index is the ratio of the flux from 8148–8172 Å, which is immediately blueward of the Na I doublet, to the flux from 8176–8200 Å, which includes the Na I doublet; Slesnick et al. (2006) also used a similar Na I index. The RECONS 1.5 m spectroscopy program observed 224 systems, including four targets in this sample, multiple times; Table 5 lists the standard deviations for each of the four spectral measures. The large uncertainties in the Na I and K I EWs are due in part to their closeness to uncorrected telluric absorption bands.

$H\alpha$ in emission (represented here as negative numbers in column 3 of Table 4) is generally considered a sign of youth, but for M dwarfs, the activity persists long beyond what is traditionally considered to be a young star (West et al. 2008). In addition, older stars still undergo occasional flares, so a single spectroscopic observation may overestimate their typically low-activity level. Thus, $H\alpha$ measurements provide some insight to the activity levels of M dwarfs, but are not sufficient to determine the age of a given star. With that caveat in mind, the lack of $H\alpha$ in emission is likely an indicator of advanced age (~ 1 Gyr); LP 991-84 is the only system in this sample that meets this criterion. Figure 3 plots the $H\alpha$ EWs versus $V - K_s$ colors for the systems in this sample, along with field systems from other RECONS spectroscopic results (Riedel et al. 2014) and confirmed stars in different moving groups, or associations, for comparison (Riedel et al. 2017, also telluric uncorrected). The field star trend, or that of those systems that are at least as old as the Pleiades (~ 150 Myr; Bell et al. 2016), and one standard deviation (1σ) from that trend are shown with a five-element moving-window average and standard deviation. As noted in Table 4, 2MASS 0429-3123AB and G161-71 exhibit high levels of $H\alpha$ emission; in Figure 3, they fall well below the field stars but above the T Tauri veiled emission limit (White & Basri 2003).

Sodium and potassium are both alkali metals, and their ionization balance is very sensitive to the surface gravity of the

Table 3
Photometry and Spectral Types

System Name (1)	R.A. (J2000.0) (2)	Decl. (J2000.0) (3)	V (mag) (4)	R (mag) (5)	I (mag) (6)	# Nights (7)	Phot. References (8)	Filter (9)	Var. (mmag) (10)	Var. References (11)	Flare? (12)	J (mag) (13)	H (mag) (14)	K _S (mag) (15)	Spec. Type (16)	Spec. References (17)	Joint? (18)
LP 991-84	01 39 21.72	-39 36 09.1	14.48	12.97	11.06	3	1	V	14.2	2	...	9.209	8.629	8.274	M4.5V	3	...
LHS 1363	02 14 12.56	-03 57 43.6	16.44	14.71	12.62	4	1	I	11.1	2	...	10.481	9.858	9.485	M5.5V	3	...
G75-35	02 41 15.14	-04 32 17.8	13.79	12.48	10.77	2	1	R	10.1	2	...	9.199	8.581	8.246	M4.0V	3	...
2MASS 0251-0352	02 51 15.00	-03 52 48.1	21.61	18.81	16.55	1,3,3	4	I	11.8	3	...	13.059	12.254	11.662	L3.0V	5	...
LP 888-18	03 31 30.25	-30 42 38.8	18.81	16.55	14.10	2	1	I	9.0	2	...	11.360	10.700	10.264	M8.0V	3	...
LP 889-37	04 08 55.58	-31 28 54.0	14.56	13.21	11.48	2	1	R	10.1	2	...	9.775	9.164	8.823	M4.0V	4	...
LHS 5094	04 26 32.65	-30 48 01.9	14.17	12.73	10.99	2	1	V	21.7	2	...	9.303	8.718	8.411	M4.0V	4	...
2MASS 0429-3123AB	04 29 18.43	-31 23 56.7	17.39	15.50	13.32	3	2	R	18.8	2	...	10.874	10.211	9.770	M5.5V	4	J
LP 834-32	04 35 36.19	-25 27 34.9	12.44	11.26	9.73	3,3,2	4	V	42.0	2	2011	8.240	7.646	7.406	M3.5V	3	...
LP 776-25	04 52 24.42	-16 49 22.2	11.63	10.53	9.12	3	1	V	15.6	3	...	7.740	7.146	6.891	M3.0V	3	...
2MASS 0517-3349	05 17 37.70	-33 49 03.1	19.75	17.38	14.96	3	1	I	10.4	2	...	12.004	11.317	10.832	M8.0V	3	...
LP 717-36AB	05 25 41.67	-09 09 12.6	12.59	11.43	9.92	2	1	V	15.4	2	...	8.454	7.882	7.623	M3.5V	3	J
LHS 6167AB	09 15 36.40	-10 35 47.2	13.82	12.32	10.42	3	1	V	32.2	2	2013	8.605	8.074	7.733	M4.5V	3	J
2MASS 0921-2104	09 21 14.10	-21 04 44.4	20.85	18.50	16.17	2	1	I	13.5	2	...	12.779	12.152	11.690	L1.5V	6	...
G161-71	09 44 54.18	-12 20 54.4	13.76	12.26	10.36	2	3	V	35.8	2	...	8.496	7.919	7.601	M4.5V	4	...
LP 731-76	10 58 27.99	-10 46 30.5	14.44	13.05	11.24	3	2	I	34.8	2	2006	9.512	8.965	8.640	M4.5V	3	...
LHS 2783AB	13 42 09.97	-16 00 23.4	13.42	12.14	10.52	2	1	R	16.7	2	...	8.971	8.391	8.089	M4.0V	7	J
LP 739-2	13 58 16.18	-12 02 59.1	14.46	13.10	11.39	2	1	I	10.6	2	...	9.728	9.174	8.887	M4.0V	3	...
LHS 2880	14 13 04.86	-12 01 26.8	13.89	12.52	10.79	3	1	R	14.3	2	...	9.040	8.453	8.163	M4.5V	4	...
2MASS 1507-2000	15 07 27.81	-20 00 43.3	18.82	16.70	14.29	2	2	I	9.7	2	...	11.713	11.045	10.661	M7.5V	5	...
LHS 3056	15 19 11.74	-12 45 06.7	12.87	11.63	10.04	2	1	V	10.0	3	...	8.507	7.862	7.582	M4.0V	7	...
2MASS 1534-1418	15 34 56.93	-14 18 49.2	19.15	16.71	14.16	3	1	I	8.1	2	...	11.380	10.732	10.305	M7.0V	8	...
LP 869-19AB	19 42 00.66	-21 04 05.6	13.22	11.93	10.28	3	3	R	13.2	2	...	8.692	8.079	7.816	M4.0V	3	J
LP 869-26AB	19 44 53.80	-23 37 59.4	14.09	12.65	10.85	3	1	R	11.2	2	...	9.169	8.571	8.265	M4.5V	3	J
LP 870-65	20 04 30.79	-23 42 02.4	13.02	11.75	10.09	3	1	R	13.3	2	...	8.559	8.012	7.701	M4.0V	3	...
LP 756-3	20 46 43.64	-11 48 13.3	13.80	12.52	10.88	2	1	R	18.9	2	...	9.349	8.728	8.435	M4.0V	3	...
LP 984-92	22 45 00.07	-33 15 26.0	13.37	12.06	10.33	6	4	R	20.3	3	...	8.681	8.057	7.793	M4.5V	3	...
Fomalhaut C	22 48 04.50	-24 22 07.8	12.59	11.31	9.61	3	9	V	12.0	2	...	8.075	7.527	7.206	M4.0V	3	...
LP 932-83	22 49 08.41	-28 51 20.1	13.94	12.67	10.98	3	1	V	46.4	2	2010	9.342	8.780	8.474	M4.0V	3	...
2MASS 2306-0502 ^a	23 06 29.36	-05 02 29.2	18.75	16.54	14.10	3	1	I	11.6	4	2009	11.354	10.718	10.296	M7.5V	5	...
LP 822-101	23 31 25.04	-16 15 57.8	13.13	11.95	10.40	3	1	V	10.4	3	...	8.877	8.290	8.004	M3.5V	3	...
2MASS 2351-2537AB	23 51 50.48	-25 37 36.7	19.98	17.86	15.47	2	1	I	9.5	2	...	12.471	11.725	11.269	M8.5V	3	J

Note. A year in the “Flare?” column indicates that a flare was detected in the astrometric frames during that year. JHK_S photometry is from 2MASS. A “J” in the “Joint?” column indicates that joint photometry and spectroscopy data are presented for a binary that neither of the CTIO/SMARTS telescopes (0.9 and 1.5 m) nor 2MASS was able to resolve.

^a Also known as TRAPPIST-1.

References. (1) Winters et al. (2015), (2) Hosey et al. (2015), (3) Bartlett (2007a), (4) this work, (5) Cruz et al. (2003), (6) Reid et al. (2008), (7) Reid et al. (1995), (8) Cruz et al. (2007), (9) Mamajek et al. (2013).

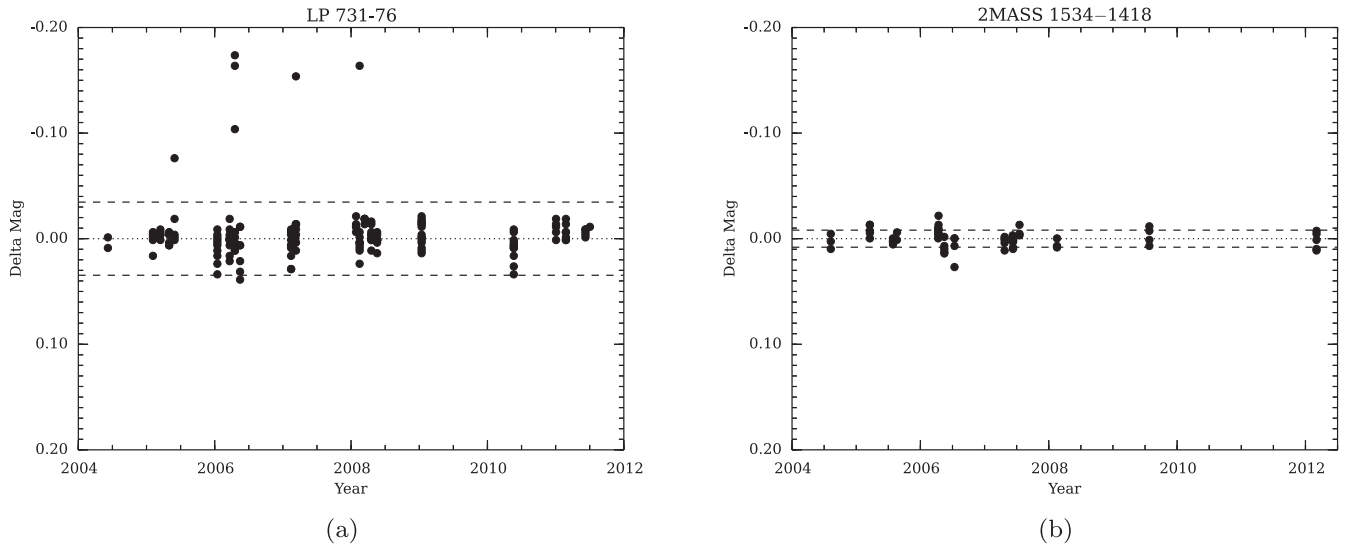


Figure 2. The light curves of LP 731-76 and 2MASS 1534-1418 are shown around their respective mean instrumental magnitudes; both systems were observed in the *I* band. LP 731-76 appears to be more variable than other systems in this sample and to have flared in 2006, while the apparent variability of 2MASS 1534-1418 is near the threshold for detectability. The standard deviation of 35 mmag for LP 731-76 is calculated using 167 images from 22 nights of observations. The standard deviation of 8 mmag for 2MASS 1534-1418 is calculated using 62 images from 15 nights of observations. Based on three nights of CTIOPI photometry each, the *I*-band magnitude of LP 731-76 is 11.24 ± 0.02 and that of 2MASS 1534-1418 is 14.16 ± 0.01 .

Table 4
Spectral Indices from the RECONS 1.5 m Spectroscopy Program and Radial Velocities from the Literature

System Name (1)	Spectral Type (2)	H α EW (\AA) (3)	Na I Index (4)	Na I EW (\AA) (5)	K I EW (\AA) (6)	Joint? (7)	Low Gravity (8)	Rad. Vel. (km s^{-1}) (9)	References (10)
LP 991-84	M4.5V	+0.25	1.29	5.52	2.86			...	
LHS 1363	M5.5V	-7.45	1.35	6.03	4.47			-15.6 ± 1.7	1
G75-35	M4.0V	-4.51	1.23	4.98	2.15			...	
2MASS 0251-0352	1.26 ± 0.13	2
LP 888-18	M8.0V	-4.61	1.35	6.16	5.99			23.4 ± 3	3
LP 889-37	M4.0V	-1.47	1.24	5.69	2.25			...	
LHS 5094	M4.0V	-6.91	1.25	5.49	2.09			...	
2MASS 0429-3123AB	M5.5V	-24.59	1.33	5.87	3.88	J	Na Idx/EW, K	39.6 ± 3	3
LP 834-32	M3.5V	-7.79	1.15	4.27	1.20		Na Idx	...	
LP 776-25	M3.0V	-5.18	1.17	4.35	1.04			27.9 ± 0.3	4
2MASS 0517-3349	M8.0V	-2.28	1.35	6.11	5.83			29.4 ± 2.8	1
LP 717-36AB	M3.5V	-4.08	1.18	4.21	1.20	J	Na EW	28.4 ± 0.5	4
LHS 6167AB	M4.5V	-3.27	1.29	5.79	3.37	J		...	
2MASS 0921-2104	80.53 ± 0.05	2
G161-71	M4.5V	-24.37	1.22	3.99	2.20		Na Idx/EW	...	
LP 731-76	M4.5V	-6.35	1.27	4.87	2.65			...	
LP 739-2	M4.0V	-0.01	1.20	4.01	2.02		Na EW	...	
LHS 2880	M4.5V	-8.36	1.20	4.84	1.48		Na Idx/EW, K	...	
2MASS 1507-2000	-2.5 ± 3	3
2MASS 1534-1418	-75.5 ± 3	3
LP 869-19AB	M4.0V	-3.81	1.27	5.31	1.81	J		...	
LP 869-26AB	M4.5V	-4.44	1.25	4.45	2.57	J	Na EW	...	
LP 870-65	M4.0V	-7.76	1.24	4.90	2.07			...	
LP 756-3	M4.0V	-5.76	1.25	4.94	1.95			-32.8 ± 0.3	4
LP 984-92	M4.5V	-9.22	1.16	3.74	1.00		Na Idx/EW, K	2.4 ± 1.0	5
Fomalhaut C	M4.0V	-3.81	1.23	5.19	2.10			6.5 ± 0.5	6
LP 932-83	M4.0V	-8.30	1.21	4.43	1.46		Na EW, K	...	
2MASS 2306-0502	-56.3 ± 3	3
LP 822-101	M3.5V	-0.04	1.20	4.42	1.03		K	...	
2MASS 2351-2537AB	M8.5V	-4.32	1.35	5.91	4.61	J		-10 ± 3	3

Note. Spectral types and indices are from this work. The uncertainty in a type is ± 0.5 subtype. Table 5 summarizes the uncertainties in H α EWs, Na I indices, Na I EWs, and K I EWs. A “J” in the “Joint?” column indicates that a joint spectral type and indices are reported for a binary that was unresolved by the CTIO/SMARTS 1.5 m.

References. (1) Deshpande et al. (2012), (2) Blake et al. (2010), (3) Reiners & Basri (2009), (4) Shkolnik et al. (2012), (5) Torres et al. (2006), (6) Mamajek et al. (2013).

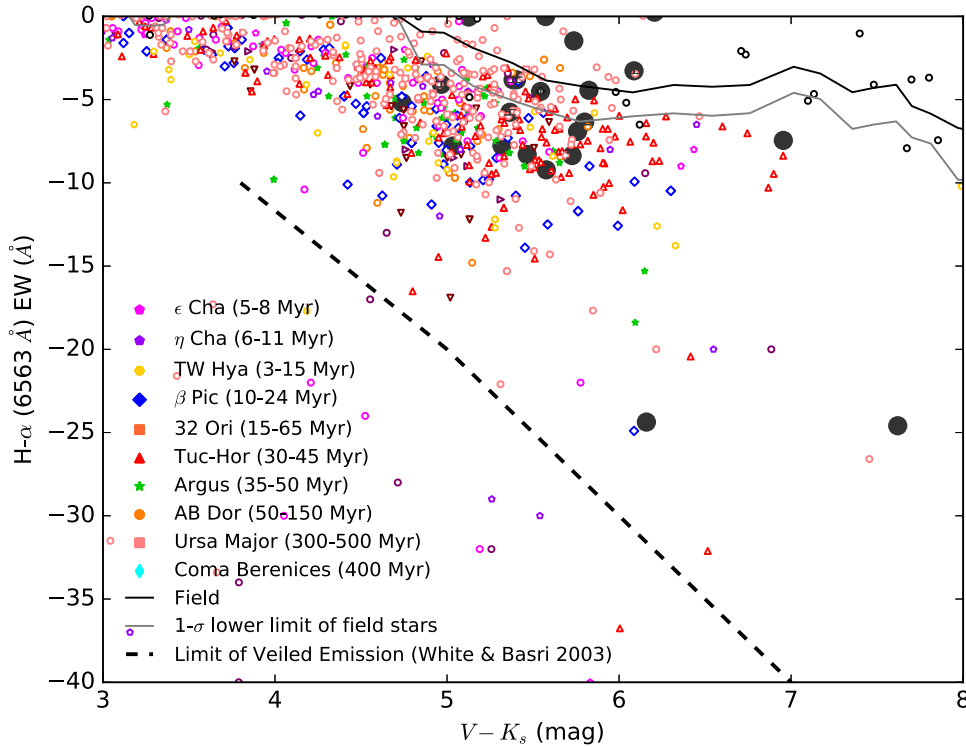


Figure 3. A plot of $H\alpha$ EW vs. $V - K_s$ color for the systems in this sample with RECONS spectroscopy (filled black circles). For comparison, the open black circles are field systems from other RECONS spectroscopic holdings. A five-element moving-window average (solid black line) and corresponding moving-window standard deviation (solid gray line) demonstrate the trend for field stars, which are at least as old as the Pleiades. Known young systems (Riedel et al. 2017) are plotted in colors identifying the moving group, or association, to which they belong. The T Tauri veiled emission limit (White & Basri 2003) is shown with a dashed curve. The ages of the moving groups and open clusters are as reported in Riedel et al. (2017).

Table 5
Standard Deviations for Spectral Indices from RECONS
1.5 m Spectroscopy Program

System Name (1)	Standard Deviations				Joint? (6)
	$H\alpha$ EW (\AA) (2)	Na I Index (3)	Na I EW (\AA) (4)	K I EW (\AA) (5)	
LHS 2880	0.06	0.01	0.32	0.13	...
LP 869-26AB	0.55	0.01	0.60	0.31	J
LP 776-25	0.34	0.05	1.05	0.20	...
LHS 6167AB	0.13	0.01	0.05	0.22	J
Sample Median	0.24	0.01	0.46	0.21	...
RECONS Median	0.16	0.02	0.46	0.33	...

Note. Sample median is the median of the standard deviations of the four systems in this sample for which multiple spectra were available. RECONS median is the median of the standard deviations of all 224 systems observed multiple times by the RECONS 1.5 m spectroscopy program. A “J” in the “Joint?” column indicates that joint spectroscopy data are presented for a binary that was unresolved by the CTIO/SMARTS 1.5 m telescope.

star (Allers et al. 2007) and therefore to its physical radius. As noted in Schlieder et al. (2012), pre-main-sequence M dwarfs younger than the Pleiades are still notably enlarged and exhibit measurably weaker neutral sodium features, indicative of their low surface gravities. Neutral potassium features are similarly weaker. Like the $H\alpha$ plot in Figure 3, Figures 4–6 plot the Na I index, Na I EW, and K I EW, respectively, versus $V - K_s$ colors for the 25 systems in this sample for which we have spectra along with the comparison subsets of stars. Systems are

identified as potentially young in these plots if they lie below the 1σ limit shown in gray in each plot. The Na I index is a better discriminator of youth than its corresponding EW. Ten systems demonstrate lower than normal gravity according to at least one of these three measures: 2MASS 0429-3123AB, LP 834-32, LP 717-36AB, G161-71, LP 739-2, LHS 2880, LP 869-26AB, LP 984-92, LP 932-83, and LP 822-101. These systems are noted as surpassing the 1σ limits for these indicators in columns 3–5 of Table 6 with the letter “Y.”

4. Discussion

Figure 7 shows the 32 targets discussed here with red points on a color–absolute magnitude diagram, i.e., an observational Hertzsprung–Russell (H-R) diagram. For comparison, the plot includes previously published π_{trig} from CTIOPI shown with black points (Jao et al. 2005, 2011, 2014; Henry et al. 2006; Riedel et al. 2010; Mamajek et al. 2013; Dieterich et al. 2014; Lurie et al. 2014; Davison et al. 2015; Benedict et al. 2016; Winters et al. 2017). The systems in this sample, especially the bluer members, appear to be elevated compared to the general trend of the main sequence. The selection process gave preference to the closest candidates among systems thought to be nearby based on existing photometric and spectroscopic estimates of distance. This approach produces a rich sample of unresolved multiples, young stars, and/or stars of high metallicity because the brighter targets were selected, resulting in systems that are preferentially elevated on the H-R diagram. In general, the distance discrepancies identified in Table 7 can be explained by unresolved companions and/or young single stars. Although exploring the metallicity of this sample further requires additional measurements, metallicity alone is unlikely to explain the full extent to which these systems

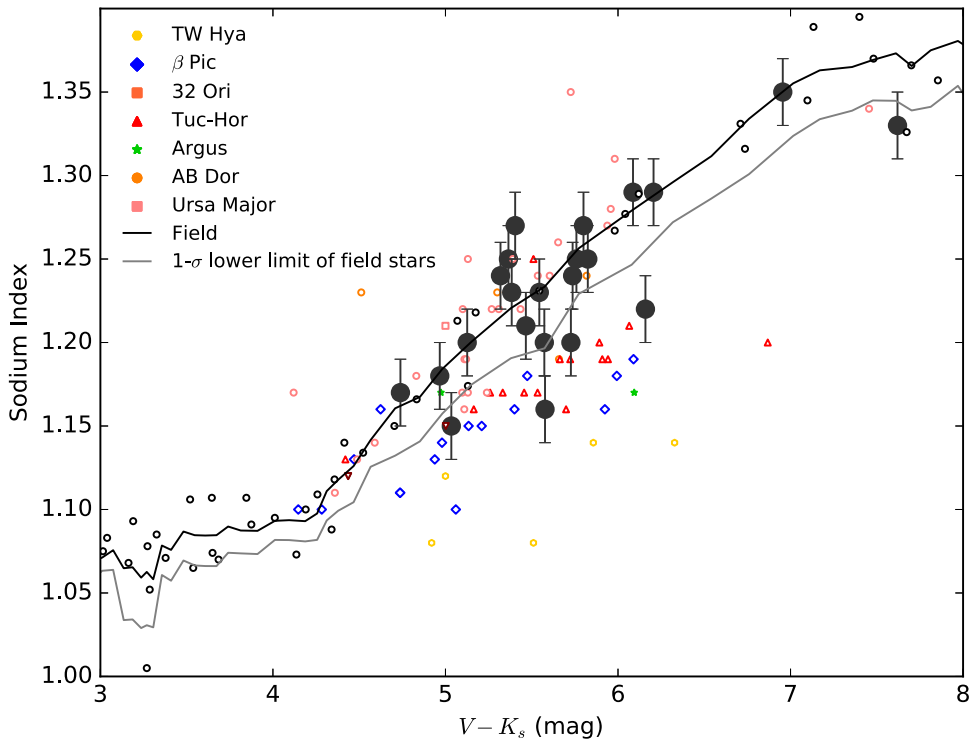


Figure 4. A plot of Na I index vs. $V - K_s$ color for the systems of this sample with RECONS spectroscopy (filled black circles). For comparison, the open black circles are field systems from other RECONS spectroscopic holdings. A five-element moving-window average (solid black line) and corresponding moving-window standard deviation (solid gray line) demonstrate the trend for field stars, which are at least as old as the Pleiades. In addition, known young systems (Riedel et al. 2017) are plotted in colors identifying the moving group or association to which they belong.

are elevated above the main sequence, in the most extreme cases by ~ 2 mag in M_V . Section 4.1 discusses binaries, including those that have been resolved by larger instruments and those that are suggested by astrometric perturbations. Section 4.2 discusses systems that appear young in the RECONS spectroscopy or by association with known young moving groups. The systems in this sample are all located in Earth’s southern hemisphere, which also contains many young moving groups and associations, so the presence of young systems is not unexpected.

4.1. Binaries and the Multiplicity Fraction

Discarding Fomalhaut C, which is the tertiary in a system with an A-star primary, we find that nine of the 31 remaining systems in this sample are binaries with red-dwarf primaries, including:

1. two wide common proper motion pairs—LP 984-91/92 and LTT 9210/LP 932-83 (Table 8),
2. five resolved systems with separations less than $1''$ —2MASS 0429-3123AB, LP 717-36AB, LHS 6167AB, LHS 2783AB, and LP 869-26AB (Table 9),
3. one double-lined spectroscopic binary (SB2)—LP 869-19AB (Malo et al. 2014),
4. one with an obvious astrometric perturbation in our data, shown in Figure 1(a)—2MASS 2351-2537AB.

However, LP 731-76 does not appear to be physically related to BD-10°3166 (Table 8). Thus, the multiplicity rate is 29% for this sample, which is consistent with multiplicity rates for M dwarfs from large surveys, e.g., $26\% \pm 3\%$ from Delfosse et al. (2004).

The selection of bright systems that photometric or spectroscopic distance estimates placed nearby under the assumption that they were single stars potentially biased the sample to include unresolved multiples that could yield a surplus of binaries. As outlined in Table 7, remaining offsets between trigonometric and photometric/spectroscopic distances for a few more targets indicate that some may be unresolved multiples awaiting resolution in the future with high-resolution techniques, e.g., speckle imaging, adaptive optics, or radial-velocity monitoring.

4.2. Youth and Activity

The results of our youth analysis are summarized for each of the 32 systems in Table 6. Nearby M dwarfs may still be pre-main-sequence stars undergoing gravitational collapse on their way to the zero-age main sequence, and as such would appear more luminous than ordinary field stars. Six members of the sample display clear overluminosity in Figure 7, and several others lie above the median line of other stars observed during CTIOPI. As discussed in Section 4.1, multiplicity can explain some of these brighter systems, but another alternative is that these systems are young.

Although the RECONS spectroscopic measurements have large uncertainties, a few of the systems appear to be young based on the measurements presented here. Five systems lie below the main-sequence locus in Figures 4–6, in at least two of the three plots, suggesting ages less than 120 Myr: G161-71, which is shown below to be a possible member of Argus Association; LP 984-92, which is confirmed below as a member of the β Pictoris (β Pic) Moving Group; and 2MASS

Table 6
Indicators of Stellar Youth

System Name (1)	Flags						LACEwING		BANYAN II		Final Call	
	H α (2)	Na Idx (3)	Na EW (4)	K EW (5)	Varia. (6)	HRD (7)	Group (8)	Prob. (9)	Group (10)	Prob. (11)	Young? (12)	Member (13)
LP 991-84	N	N	N	N	N	MS	None		Old	73.5	No	
LHS 1363	Y	N	N	N	N	MS	None		Old	100	No	
G75-35	N	N	N	N	N	MS	Argus	35	Argus	91	Young	Argus
2MASS 0251-0352	N	MS	None		Old	100	No	
LP 888-18	N	N	N	N	N	MS	AB Dor	75	Old	90	Maybe	AB Dor?
LP 889-37	N	N	N	N	N	MS	None		Old	78	No	
LHS 5094	Y	N	N	N	Y	MS	None		Old	90	No	
2MASS 0429-3123AB	Y	Y	Y	Y	N	OL	None		Old	100	Young	Unknown
LP 834-32	Y	Y	N	N	Y	MS	AB Dor	84	AB Dor	96	Young	AB Dor
LP 776-25	Y	N	N	N	N	MS	AB Dor	75	AB Dor	100	Young	AB Dor
2MASS 0517-3349	N	N	N	N	N	MS	None		Old	100	No	
LP 717-36AB	Y	N	Y	N	N	MS	AB Dor	51	AB Dor	100	Young	AB Dor
LHS 6167AB	N	N	N	N	Y	MS	None		Old	66	No	
2MASS 0921-2104	N	MS	None		Old	100	No	
G161-71	Y	Y	Y	N	Y	OL	Argus	53	Argus	99	Young	Argus
LP 731-76	Y	N	N	N	Y	MS	None		Old	72	No	
LHS 2783AB	N	MS	None		Old	91	No	
LP 739-2	N	N	Y	N	N	MS	None		Old	100	No	
LHS 2880	Y	Y	Y	Y	N	OL	None		Old	100	Young	Unknown
2MASS 1507-2000	N	OL	None		Old	72	No	
LHS 3056	N	OL	None		Old	100	No	
2MASS 1534-1418	N	MS	None		Old	100	No	
LP 869-19AB	N	N	N	N	N	OL	None		β Pic	75	No	
LP 869-26AB	N	N	Y	N	N	MS	None		Old	82	No	
LP 870-65	Y	N	N	N	N	OL	AB Dor	39	AB Dor	99	Young	AB Dor
LP 756-3	Y	N	N	N	N	MS	None		Old	86	No	
LP 984-92	Y	Y	Y	Y	Y	OL	β Pic	100	β Pic	100	Young	β Pic
Fomalhaut C	N	N	N	N	N	MS	None		Old	59	No	
LP 932-83	Y	N	Y	Y	Y	OL	None		Old	100	Young	Unknown
2MASS 2306-0502 ^a	N	MS	None		Old	100	No	
LP 822-101	N	N	N	Y	N	OL	None		Old	100	Maybe	Unknown?
2MASS 2351-2537	N	N	N	N	N	OL	None		Old	90	No	

Note. A “Y” denotes one of the following conditions: greater 1σ activity in H α 6563 Å EW; greater than 1σ youth based on Na I 8200 Å doublet index (Na Idx), Na I 8200 Å doublet EW (Na EW), or K I 7699 Å EW (K EW); or variability of 20 mmag or more. A system’s position on the observational H-R diagram in Figure 7 is identified as either on the main sequence (MS) or as overluminous (OL).

^a Also known as TRAPPIST-1.

0429-3123AB, LHS 2880, and LP 932-83, which appear to be young systems not associated with any cluster or association.

In addition to indicators of young systems above, a number of the π_{trig} targets are suggested to be members of nearby young moving groups (e.g., Torres et al. 2006, 2008; Shkolnik et al. 2012; Malo et al. 2013). These moving groups are low-density, loose associations of stars that formed from a single burst of star formation. Although they are in the process of dispersing into the general disk population, at the moment they are young enough (5–300 Myr) that they still retain much of the original space velocity of the gas from which they formed. Studying the kinematics of the systems can identify members of the nearby young moving groups. The LocAting Constituent mEmbers In Nearby Groups code (Riedel 2016; Riedel et al. 2017, hereafter LACEwING)¹⁶ processes any available astrometric information to determine the probable space velocities and memberships of the systems, with increasing accuracy as more data are available. LACEwING determines and combines up to four kinematic criteria, based on the information available.

1. Proper Motions. For a given right ascension (R.A.) and declination (decl.), the appropriate proper motion angle of a member of a given moving group can be calculated and compared to known proper motions. The CTIOPI positions and astrometry in Table 1 provide the relevant information.
2. Distances. The magnitude of the proper motion vector (calculated above) can be used to derive a kinematic distance to the star, which LACEwING compares to the distance derived from the CTIOPI π_{trig} .
3. Spatial Position. While less useful as a discriminant, LACEwING uses the CTIOPI-provided position and π_{trig} to determine whether the spatial location of the star is appropriate for a given moving group.
4. Radial Velocity. When available, a measured radial velocity can be compared to an estimated radial velocity calculated with the kinematic proper motion above. Although RECONS spectra are insufficient for radial velocity determination, other groups have published radial velocities for several of these systems. Table 4

¹⁶ <https://github.com/ariedel/lacewing>

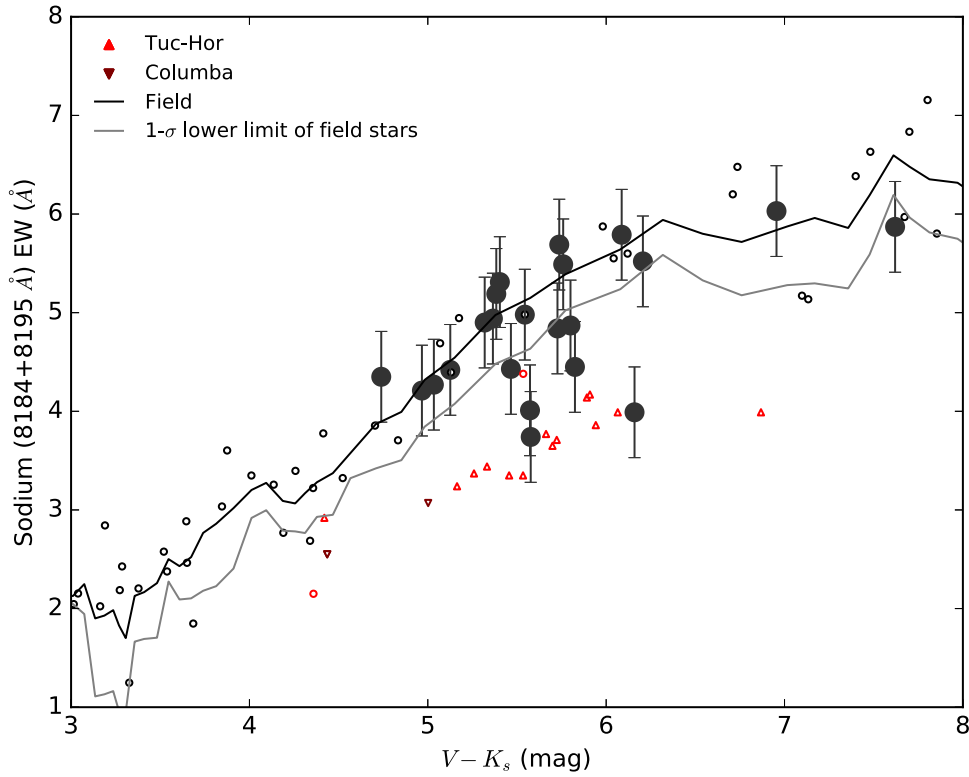


Figure 5. A plot of Na I EW vs. $V - K_s$ color for the systems of this sample with RECONS spectroscopy (filled black circles). For comparison, the open black circles are field systems from other RECONS spectroscopic holdings, which are at least as old as the Pleiades. A five-element moving-window average (solid black line) and corresponding moving-window standard deviation (solid gray line) demonstrate the trend for field stars. In addition, known systems from Riedel et al. (2017) (incorporated from Shkolnik et al. 2009 and Riedel et al. 2014, which also did not make telluric corrections) are plotted in colors identifying the moving group or association to which they belong.

Table 7
Comparison of Trigonometric, Photometric, and Spectroscopic Distances

System Name	Trigonometric (pc)	Photometric (pc)	References	Spectroscopic (pc)	References	Variable?	Notes
(1)	(2)	(3)	(4)	(5)	(6)	(7)	(8)
2MASS 0429-3123AB	17.0 ± 0.4	11 ± 2	1	9.7 ± 0.9	2		photometry resolves components
LP 717-36AB	20.4 ± 0.6	13 ± 2	3		joint photometry
		20 ± 5	10		photometry resolves components
G161-71	13.5 ± 0.3	6.2 ± 0.5	3	7 ± 1	4	V	
LHS 2880	31 ± 1	9.8 ± 0.7	3	9 ± 3	5		
2MASS 1507-2000	23.5 ± 0.4	14 ± 1	2		
LHS 3056	21.2 ± 1.0	10 ± 2	6		
LP 869-19AB	18.6 ± 0.6	10 ± 1	7	12 ± 2	4		joint photometry, spectroscopy
LP 869-26AB	14.7 ± 0.2	9 ± 1	2	9 ± 2	4		joint photometry, spectroscopy
		13	8		photometry resolves components
LP 870-65	18.2 ± 0.5	10 ± 2	7	9 ± 2	4		
LP 984-92	21 ± 1	8 ± 1	7	V	
LP 932-83	34 ± 3	14 ± 2	3	10.2 ± 2.0	4	V	
LP 822-101	36 ± 3	14 ± 2	6	20 ± 4	4		
2MASS 2351-2537AB	21.2 ± 0.5	17 ± 3	6	18 ± 2	9		perturbation

Note. Parallax distances are from this work. Systems with “V” in the “Variable?” column demonstrated a photometric variability greater than 20 mmag during astrometric observations.

References. (1) Siegler et al. (2005), (2) Cruz et al. (2003), (3) Reid et al. (2002), (4) Scholz et al. (2005), (5) Riaz et al. (2006), (6) Winters et al. (2015), (7) Reid et al. (2003), (8) Montagnier et al. (2006), (9) Cruz et al. (2007), (10) Daemgen et al. (2007).

identifies the radial velocities used to supplement the CTIOPI astrometry.

For each system under consideration, LACEwING calculates the three (or four) metrics for each of the 16 moving groups,

open clusters, and associations it considers: ϵ Chamaeleontis, η Chamaeleontis, TW Hydrae, β Pic, 32 Orionis, Octans, Tucana–Horologium, Columba, Carina, Argus, AB Doradus (AB Dor), Carina-near, Coma Berenices, Ursa Major, χ 01 Fornacis, and Hyades. Then, LACEwING combines the

Table 8
Evaluation of Wide Common Proper Motion Pairs

Name (1)	R.A. (J2000.0) (2)	Decl. (J2000.0) (3)	π (abs) (mas) (4)	μ (mas yr ⁻¹) (5)	P.A. (deg) (6)	References (7)	V (mag) (8)	References (9)	K_S (mag) (10)	Mass (M_{\odot}) (11)	Spectral Type (12)	References (13)	Physically Related? (14)
LP 731-76	10 58 27.99	-10 46 30.5	73.22 ± 1.69	212.3 ± 0.8	248.0 ± 0.37	1	14.44	1	8.640	0.18 ± 0.04	M4.5V	1	
BD -10° 3166	10 58 28.79	-10 46 13.4	15.34 ± 3.082	185.9 ± 1.5	269.1 ± 0.67	2	10.03	2	8.124	0.8 ± 0.2	K3.0V	2	No
LP 984-92	22 45 00.07	-33 15 26.0	47.84 ± 2.34	215.0 ± 0.9	122.9 ± 0.49	1	13.37	1	7.793	0.41 ± 0.05	M4.5V	1	
LP 984-91	22 44 57.97	-33 15 01.7	42.84 ± 3.61	220.2 ± 3.5	123.0 ± 1.76	3	12.1	4	6.932	0.63 ± 0.06	M4.5V	5	Yes
LP 932-83	22 49 08.41	-28 51 20.1	29.79 ± 2.09	296.2 ± 0.9	218.4 ± 0.33	1	13.94	1	8.474	0.48 ± 0.05	M4.0V	1	
LTT 9210	22 48 52.95	-28 50 03.0	24.91 ± 2.19	295.6 ± 2.9	215.3 ± 1.1	3	10.668	6	7.083	0.7 ± 0.2	K7V	7	Yes

Note. Masses for M and K dwarfs are calculated using the mass- K_{CIT} relationship defined by references 8 and 9, respectively, after transforming the 2MASS K_S values to the California Institute of Technology (CIT) system defined by reference 10 using the equations of reference 11.

References. (1) This work, (2) Lurie et al. (2014), (3) van Leeuwen (2007), (4) Koen et al. (2010), (5) Shkolnik et al. (2009), (6) ESA (1997) and Høg et al. (2000), (7) Upgren et al. (1972), (8) Delfosse et al. (2000), (9) Henry & McCarthy (1993), (10) Elias et al. (1982), (11) Carpenter (2006).

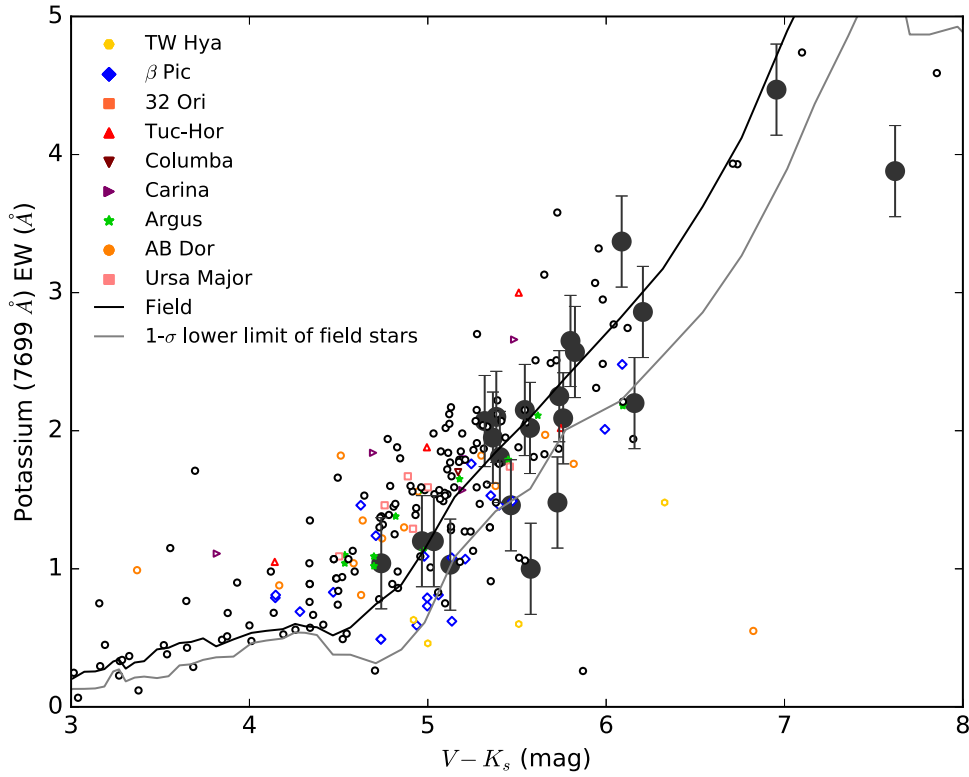


Figure 6. A plot of K I EW vs. $V - K_s$ color for the systems of this sample with RECONS spectroscopy (filled black circles). For comparison, the open black circles are field systems from other RECONS spectroscopic holdings. A five-element moving-window average (solid black line) and corresponding moving-window standard deviation (solid gray line) demonstrate the trend for field stars, which are at least as old as the Pleiades. In addition, known young systems (Riedel et al. 2017) are plotted in colors identifying the moving group or association to which they belong.

Table 9
Observations of Resolved Binaries with Separations $<1''$

System Name (1)	Separation (arcsec) (2)	Position Angle (deg) (3)	Epoch (4)	Reference (5)
2MASS 0429-3123AB	0.531 ± 0.002	298.9 ± 0.2	2003 Feb 13	1
	0.55	287.0	2005	2
LP 717-36AB	0.527 ± 0.002	69.40 ± 0.11	2005 Oct 14	3
	0.616 ± 0.004	58.8 ± 0.3	2008 Nov 10	4
	0.47 ± 0.04	56 ± 1	2010 Nov 16	5
LHS 6167AB	0.076 ± 0.001	82.4 ± 0.3	2003 Sep 12	6
	0.172 ± 0.001	265.8 ± 0.1	2005 May 1	6
	0.123 ± 0.003	175.7 ± 1.4	2012 Feb	7
LHS 2783AB	0.513	82.5	2008 Jun 16	8
	0.504	71.5	2010 Jan 26	8
	0.501	67.6	2010 Aug 4	8
	0.566	44.1	2014 Mar 9	9
LP 869-26AB	0.813 ± 0.005	354.7 ± 0.3	2004 Jul 3	6
	0.828 ± 0.005	353.1 ± 0.1	2005 Oct 14	6
	0.790	347.9	2010 Aug 5	8

References. (1) Siegler et al. (2005), (2) Reid et al. (2006), (3) Daemgen et al. (2007), (4) Bergfors et al. (2010), (5) Shkolnik et al. (2012), (6) Montagnier et al. (2006), (7) Janson et al. (2014), (8) B. Mason (2015, private communication), (9) Tokovinin et al. (2015).

metrics and transforms them into membership probabilities using precomputed membership probability functions, derived from a simulation of the solar neighborhood. LACEwING has

two sets of precomputed membership probability functions: one assumes that systems are drawn from a general field population and one assumes that the systems are known to be

young. For each group, LACEwING combines the systems's metrics into a goodness-of-fit match. Based on a large simulation of the solar neighborhood, LACEwING knows the percentage of simulated stars at the same goodness-of-fit value that are actual members of the group and reports this value as the membership likelihood for the system. LACEwING considers field stars to be 50 times more common than group members, so its estimates are accurate in that regard.

The LACEwING analysis was run twice, once in each mode with preference being given to the results from the young-star mode, if the available spectroscopic indices suggested a particular system may be young. LACEwING identifies LP 984-92 as a member of the β Pic Moving Group and LP 888-18, LP 834-32, and LP 776-25 as members of the AB Dor Moving Group. It also suggests the possibility that G75-35 and G161-71 could belong to Argus, and that LP 717-36AB and LP 870-65 could belong to AB Dor. Table 6 lists the resulting membership probabilities, while Section 5 discusses individual systems. The ages of the β Pic, Argus, and AB Dor groups and their constituent stars are 10–24, 35–50, and 50–150 Myr, respectively (Riedel et al. 2017).

Of the eight systems LACEwING associated with young moving groups or associations, all of the available spectroscopic indices identified one of them as a young system: LP 984-92 in β Pic. Although three systems identified with the AB Dor Moving Group do not appear to be low-gravity objects in any of the available spectroscopic indices, as an older association, its members are probably too old to show such features. LACEwING did not identify 2MASS 0429-3123, LHS 2880, LP 932-83, or LP 822-101 with any moving group or association in either mode although their Na I index or K I EW suggests that they are young systems. These four systems should be investigated further; in particular, because most of these systems do not have a radial velocity measurement, obtaining those values may clarify the group to which each belongs or whether perhaps they belong to a yet unidentified group.

For comparison, the Bayesian Analysis for Nearby Young AssociationNs II (version 1.4) code (Malo et al. 2013; Gagné et al. 2014, hereafter BANYAN II)¹⁷ was also used to analyze the CTIOPI astrometry and radial velocities from the literature, treating each system both as a field system and as a young system. Table 6 reports the BANYAN II results as well; again, preference is given to results from the young-star mode only when the system appears to be young in the available spectroscopy. In all but two cases, LACEwING and BANYAN II assign systems to the same population, field, or young moving group, although BANYAN II membership probabilities indicate a greater degree of certainty than LACEwING probabilities. LACEwING identifies LP 888-18 with the AB Dor Moving Group while BANYAN interprets it as a field system. LP 888-18 does not appear to have lower than normal gravity in any of the spectroscopic indices available, but that is consistent with other members of the AB Dor Moving Group identified herein. BANYAN II identifies LP 869-19AB as a member of β Pic while LACEwING considers it a field system. As discussed in Section 5, this system does not appear to have lower than normal gravity either. Because BANYAN II assumes that field stars outnumber moving-group members by only 4 to 1, its false

positive rate should be higher than that of LACEwING, which adopts a 50:1 ratio.

Previous investigations have considered the possibility that at least six systems in this sample are members of moving groups or open clusters. Similar to this LACEwING analysis, Malo et al. (2013) and Shkolnik et al. (2012) identified LP 984-92 as a member of the β Pic Moving Group and identified LP 776-25 and LP 717-36AB with the AB Dor Moving Group. In addition, LACEwING agrees with Malo et al. (2013) about LP 834-32 belonging to the AB Dor and G161-71 to the Argus Association. However, Malo et al. (2013) consider LP 869-19AB a strong AB Dor candidate, while LACEwING assigns this system to the field.

5. Notes on Individual Systems (Listed by R.A.)

01 39—LP 991-84 is one of three recent additions to the 10 pc sample in this study. Our $\pi_{\text{trig}} = 115.90 \pm 1.33$ mas is consistent with that of 113.69 ± 0.54 mas reported by Weinberger et al. (2016). It is the only star of the 25 observed by RECONS that entirely lacks H α emission, indicating that it is an old star, which is consistent with all of the youth indicators (Table 6).

02 41—G75-35 is a new candidate member of the Argus Association by LACEwING and BANYAN II as discussed in Section 4.2.

02 51—2MASS 0251-0352 is the intrinsically faintest star in this sample. It was identified as type L3V by Cruz et al. (2003), but the H-R diagram in Figure 7 suggests its color is bluer than average for that spectral type. Its color appears to be more consistent with that of an \sim L1V system; additional spectroscopy would confirm its spectral type and determine whether it is earlier than the end of the hydrogen-burning limit of main-sequence stars. Although it appears to be on the lower edge of the main sequence and has a relatively large tangential velocity of 112 km s^{-1} , Schmidt et al. (2015) detected H α emission, implying that it is unlikely to be an old subdwarf. As shown in Table 2, the CTIOPI μ is consistent with that measured by others (Deacon et al. 2005; Schmidt et al. 2007; Jameson et al. 2008).

03 31—LP 888-18 is an apparently single M8.0V star at 12.5 pc that is a new candidate member of the AB Doradus Moving Group according to LACEwING.

04 29—2MASS 0429-3123AB (WDS J04293-3124AB) has been resolved as a low-mass binary by the Very Large Telescope and by the *Hubble Space Telescope* (HST) (Siegler et al. 2005; Reid et al. 2006), with a separation of $\sim 0''.5$ (Table 9). At a distance of 17.0 pc, the projected separation is ~ 9 au. As discussed in Section 3.4, the binary has significant H α emission and demonstrates lower than normal gravity in all three available indices. We suspect that the binary is young, although LACEwING did not match the system to any known moving group or association.

04 35—LP 834-32 (2MASS 0435-2527) is an apparently single M3.5V star that is a possible member of the AB Dor Moving Group, indicated by both LACEwING and Malo et al. (2013). The star also shows significant variability at a level of 42 mmag in the Vband, including a flare in 2011.

04 52—LP 776-25 (TYC 5899-26-1, NLTT 14116, 2MASS 0452-1649) has been previously identified as a member of AB Dor moving group (Torres et al. 2008; Schlieder et al. 2010; Shkolnik et al. 2012; Malo et al. 2013), which is confirmed by LACEwING. Despite a previous report of two components

¹⁷ <http://www.astro.umontreal.ca/~gagne/banyanII.php>

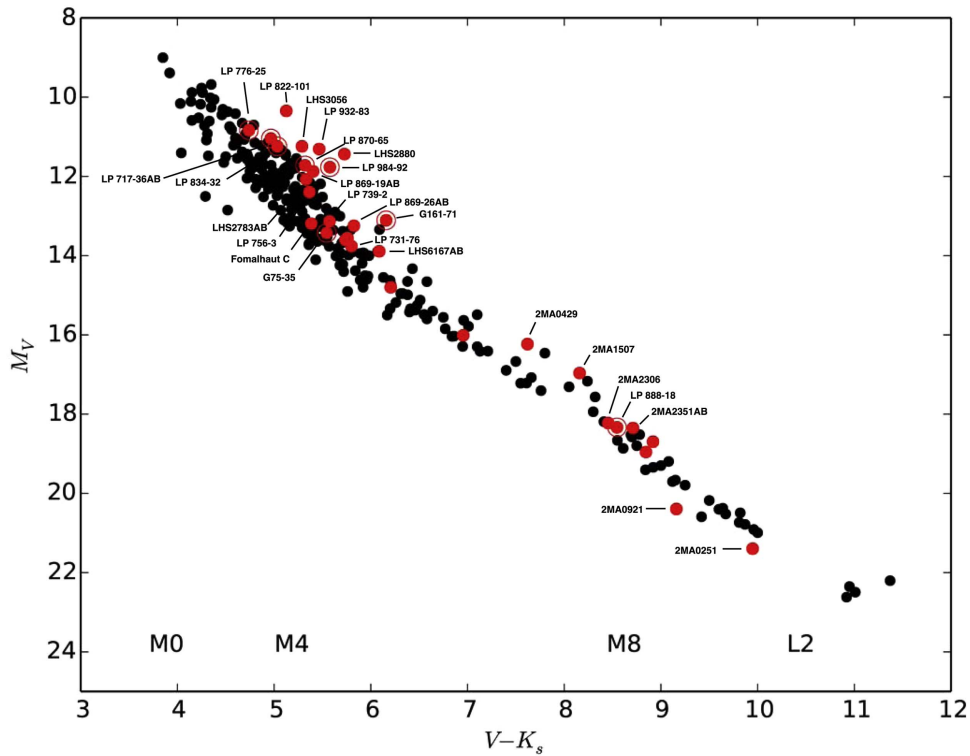


Figure 7. An observational color–absolute magnitude diagram of nearby stars highlights the systems of this sample in red. For comparison, the black dots represent stars within 25 pc reported by CTIOPI in the past (Jao et al. 2005, 2011, 2014; Henry et al. 2006; Riedel et al. 2010; Mamajek et al. 2013; Dieterich et al. 2014; Lurie et al. 2014; Davison et al. 2015; Benedict et al. 2016; Winters et al. 2017). The absolute magnitude and color errors are smaller than the size of symbols used.

(Shkolnik et al. 2009), the star is not resolved in CTIOPI frames nor was any perturbation detected in the astrometric residuals; G. Anglada-Escudé (2014, private communication) now considers it to be a single star.

05 25—LP 717-36AB (2MASS 0525-9091AB, WDS J05257-0909AB, NLTT 15049AB) is a known low-mass binary (Daemgen et al. 2007; Bergfors et al. 2010; Shkolnik et al. 2012) at a distance of 20.4 pc with a typical separation of $\sim 0''.5$ (Table 9). The binary is not resolved in CTIOPI frames nor is a perturbation seen in the astrometric residuals. The projected separation is ~ 10 au, implying a long orbital period. This system has been identified as a possible member of the AB Dor Moving Group by Shkolnik et al. (2012), Malo et al. (2013), and LACEwing. Its Na I EW demonstrates lower than normal gravity (Table 4).

09 15—LHS 6167AB (WDS J09156-1036AB) was reported in Finch & Zacharias (2016) to have $\pi_{\text{trig}} = 134.9 \pm 12.1$ mas. We provide a more accurate parallax here, $\pi_{\text{trig}} = 103.3 \pm 1.00$ mas, placing the binary just closer than 10 pc. The system has been resolved by various groups (Montagnier et al. 2006; Janson et al. 2014, see Table 9) with a typical separation of $\sim 0''.1$, implying a projected separation of ~ 1 au and orbital period of a few years. We detect perturbations of the photocenter in *V*-band images on both axes, as shown in Figure 1(c), although more data are needed to confirm a possible orbital period of ~ 4 yr, which is complicated by astrometry data acquired in both *V* filters. This system is the most promising opportunity in the sample for an accurate mass measurement in the near future.

LHS 6167AB demonstrated significant variability of 32.2 mmag in the *V* band, including a flare in 2012.

09 44—G161-71 (2MASS 0944-1220) appears to be a single M4.5V star at a distance of 13.5 pc, which is about twice its earlier photometric (6.2 pc) and spectroscopic (7 pc) distance estimates listed in Table 7. As discussed in Section 4.2, this system is a possible kinematic match for the Argus Association, which has an age of 30–50 Myr. In addition, its Na I index and EW indicate that it is a low-gravity star. It also shows significant *V*-band variability (36 mmag) and H α emission. We find it to be too bright to be a single Argus star, because it is elevated by ~ 2 mag in the H-R diagram (Figure 7); Malo et al. (2013) also consider this system overluminous for Argus. Therefore, G161-71 may be an equal-luminosity young binary. However, CTIOPI neither resolved it nor detected any indication of a perturbation in the astrometric residuals, implying an equal-luminosity double that results in no photocentric motion.

10 58—LP 731-76 was erroneously identified as a common proper motion companion to BD $-10^\circ 3166$ by Luyten (1977, 1980), the latter star having subsequently garnered much attention as an extrasolar planet host (Butler et al. 2000). Together, LP 731-76 and BD $-10^\circ 3166$ are also known as LDS 4041 or WDS J10585-1046AB. As shown in Table 8, the two proper motions do not match and π_{trig} for BD $-10^\circ 3166$ places it at a distance of 70 pc (Lurie et al. 2014), much farther than the 13.7 pc measured for LP 731-76. As discussed in Section 3.3 and illustrated in Figure 2(a), LP 731-76 demonstrated significant variability in the *I* band (35 mmag), including a flare in 2006.

13 42—LHS 2783AB (WDS J13422-1600AB) is a binary resolved by the Washington Speckle Interferometer and Southern Astrophysical Research (SOAR) 4.1 m telescope

(Tokovinin et al. 2015, B. Mason 2015, private communication) with a separation of $\sim 0''.5$ (Table 9). At a distance of 18.6 pc, the projected separation is ~ 9 au. Although Eggen (1993) considered this binary to be a member of the Hyades supercluster, LACEwING did not match this system with any moving group or association.

13 58—LP 739-2 has a Na I EW, suggesting that it may be a low-gravity object. However, this single spectroscopic indicator of youth is weak and no other indicators point to this being a young system (Table 6). In addition, LACEwING did not match this star with any moving group or association.

14 13—LHS 2880 (GJ 540.2) shows a large discrepancy between its trigonometric distance (30.9 pc) and its photometric (9.8 pc) and spectroscopic (9 pc) distance estimates (Table 7); it is consequently elevated by ~ 2 mag in the H-R diagram (Figure 7). Our CTIOPI images neither resolved it nor detected any perturbation, so it may be young. As discussed in Section 3.4, all of the spectroscopic indices examined suggest it may be a low-gravity object, although LACEwING did not match this star with any moving group or association.

15 07—2MASS 1507-2000 was found by Schmidt et al. (2007) to have H α in emission. Reiners & Basri (2009) and Gálvez-Ortiz et al. (2010) reported different radial velocities of -2.5 and -22.2 km s $^{-1}$, respectively, in measurements separated by less than one year. Based on its slightly elevated position on the H-R diagram (Figure 7) and changing radial velocity, it is possibly a binary. The star is not resolved in CTIOPI data nor is any perturbation seen (Figure 1(b)).

15 19—LHS 3056 shows a significant mismatch between trigonometric (21.2 pc) and photometric (10 pc) distances, and therefore appears elevated on the H-R diagram. LACEwING does not identify it with any moving group or association. We suspect that this star is overluminous because of an unseen companion, although no convincing perturbation is seen in our astrometric data, possibly because the two stars are nearly equal in luminosity.

19 42—LP 869-19AB was identified as an overluminous member of the AB Dor Moving Group (Malo et al. 2013), which was then found by Malo et al. (2014) to be an SB2. LACEwING did not identify it with any young moving group or association, but BANYAN II assigned it to β Pic. BANYAN II probably misidentified this system because the program assumes that field stars outnumber moving-group members by only 4 to 1.

19 44—LP 869-26AB (WDS J19449-2338AB) is a binary resolved by Montagnier et al. (2006), B. Mason (2015, private communication), and Tokovinin et al. (2015) with a separation of $\sim 0''.8$. Our CTIOPI images show an elongated source with an estimated separation of $\sim 0''.7$ (Bartlett 2007a, 2007b). At a distance of ~ 14.7 pc, the projected separation is about 12 au. Although its Na I EW suggests that LP 869-26AB is a possible low-gravity object, this single spectroscopic indicator of youth is weak and no other indicators point to this being a young system (Table 6).

20 04—LP 870-65 appears to be a single M4.0 dwarf at a distance of 18.2 pc, which is about twice its photometric (10 pc) and spectroscopic (9 pc) distance estimates (Table 7). While such a discrepancy is suggestive of an unresolved binary, CTIOPI neither resolved it nor detected any indication of a perturbation in the astrometric residuals. LACEwING identifies this star as a possible candidate for membership in AB Dor.

20 46—LP 756-3 (NLTT 49856) appears to be a single star according to radial velocity results in Shkolnik et al. (2009). They estimated its age to be 40–300 Myr based on its neutral helium (He I) emission, and later Shkolnik et al. (2012) suggested that LP 756-3 may belong to the Hyades Moving Group. LACEwING does not match this star to any moving group or association, nor do our spectroscopic indices suggest it is a young star.

22 45—LP 984-92 (GJ 871.1B, TX PsA, HIP 112312B) was identified as a common proper motion companion to LP 984-91 (GJ 871.1A, WW PsA, HIP 112312) by Luyten (1941, 1980); together, they are also known as LDS 793 or WDS J22450-3314AB. LP 981-91 and LP 984-92 are both within the field of view in our parallax frames, but the primary LP 981-91 is usually saturated. Hence, there is no CTIOPI π_{trig} for the primary, but *Hipparcos* (van Leeuwen 2007) measured $\pi_{\text{trig}} = 42.84 \pm 3.61$ mas, so our π_{trig} confirms that the two stars are in the same system. The stars are estimated to be 12 Myr old (Song et al. 2002) and members of the β Pic Moving Group (Torres et al. 2006, 2008; Shkolnik et al. 2012; Malo et al. 2013). LP 984-92 is a low-gravity object according to all three spectroscopic indicators measured here, has H α in emission, and is variable in R (20 mmag). LACEwING concurs with the previous identifications of LP 984-92 as a member of the β Pic Moving Group. Its π_{trig} places it at 20.9 pc, a distance nearly three times its photometric estimate (8 pc). LP 984-92 is not resolved in CTIOPI frames, nor do we see any perturbation in the long-term data set, so its elevation by ~ 2 mag in the H-R diagram (Figure 7) is likely due to youth. Gershberg et al. (1999) also found LP 984-92 to be overluminous and to flare similarly to UV Ceti stars.

22 48—Fomalhaut C (LP 876-10) was identified to be a third component of the Fomalhaut system (WDS J22577-2937ABC, age 440 ± 40 Myr) based on the CTIOPI astrometry and photometry presented herein (Mamajek et al. 2013). Fomalhaut C does not appear to be itself an unresolved binary; the available astrometry is inconsistent with the companion reported in the Washington Double Star (WDS)¹⁸ catalog as WDS J22577-2937CaCb (Mason et al. 2001).¹⁹ In addition, the SOAR 4.1 m telescope was unable to resolve it in 2014 (Tokovinin et al. 2015). Mamajek et al. (2013) also considered and rejected the possibility that another high proper motion star in the field, LP 876-11, is a common proper motion companion to Fomalhaut C; LP 876-11 has no measurable π_{trig} and its μ is incompatible with Fomalhaut C. At a distance of 7.6 pc, Fomalhaut C is a member of the 10 pc sample and the closest star targeted in this study.

22 49—LP 932-83 (NLTT 54933) was identified as the common proper motion companion of LTT 9210 (CD-29° 18469, HIP 112648, NLTT 54912) by Luyten (1977, 1980); together they are also known as LDS 4999 or WDS J22489-2850AB. Both stars are within the field of view of our data, but LTT 9210 was usually saturated. Hence, while no CTIOPI π_{trig} is available for the primary, *Hipparcos* (van Leeuwen 2007) measured $\pi_{\text{trig}} = 24.91 \pm 2.19$ mas. Therefore, our π_{trig} confirms that the two stars are in the same system. Photometric (14 pc) and spectroscopic (10.2 pc) distance estimates (Table 7) for LP 932-83 indicate that it is closer than measured via our π_{trig} (33.6 pc). We did not resolve the star nor detect any perturbation in the astrometric residuals, suggesting

¹⁸ <http://ad.usno.navy.mil/wds/>

¹⁹ Based on catalog entry as of 2017 January 18.

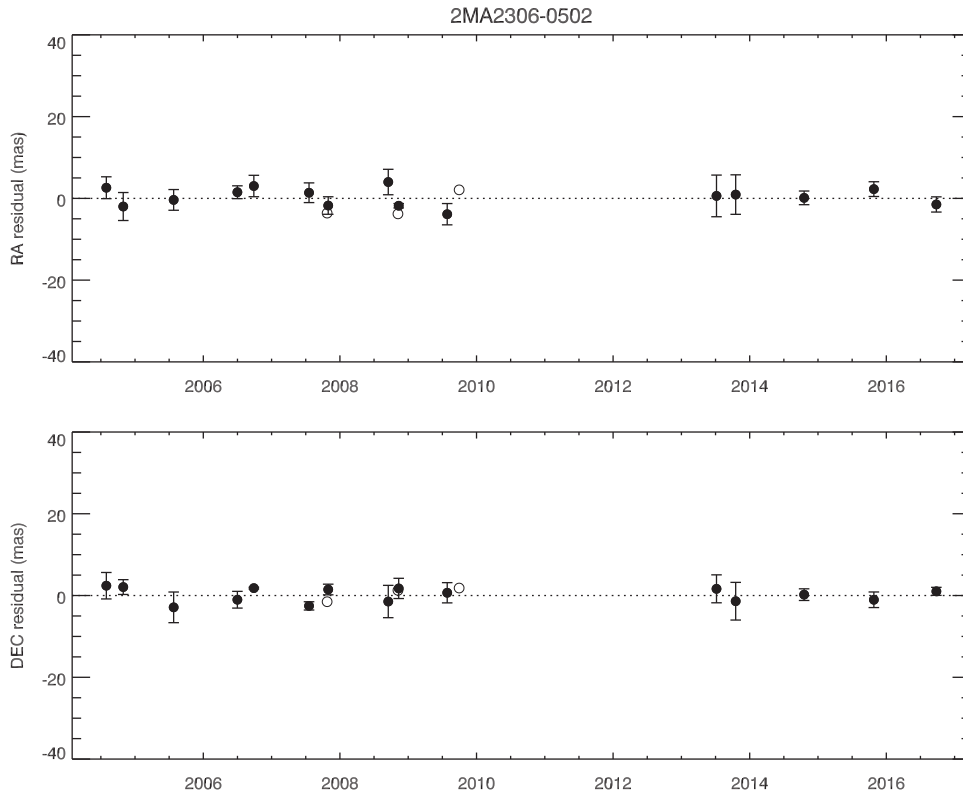


Figure 8. Nightly mean astrometric residuals in R.A. and decl. are shown for 2MASS J23062928-0502285 (TRAPPIST-1); CTIOPI detected no perturbation although the system may contain at least seven planets (Gillon et al. 2017). The astrometric signatures of the system’s μ and π_{trig} have been removed. Filled circles represent nightly means while open circles represent nights from which only one frame is available.

that the system may be an overluminous young star. This possibility is supported by two other pieces of evidence: the system varies by 46 mmag in V , including a flare in 2010, and shows lower than normal gravity in both the Na I and K I EWs. LACEwING did not match the system to any young moving group or association.

23 06—2MASS J23062928-0502285 (TRAPPIST-1) is an M7.5 dwarf first identified by Gizis et al. (2000). Later, the CTIOPI 1.5 m program measured its first π_{trig} at 82.58 ± 2.58 mas, or ~ 12.2 pc, (Costa et al. 2006) based on a 3.3 yr baseline. The CTIOPI 0.9 m program has also observed it since 2004, and we present a new parallax of 78.76 ± 1.04 mas in Table 1. Because these two parallaxes are independent measurements, we calculate its weighted mean π_{trig} to be 79.29 ± 0.96 mas, which is $\sim 4\%$ farther than the distance measured at 1.5 m. During this 12.2 yr period, we did not detect any perturbations in the astrometric residuals, which are shown in Figure 8.

Because of its proximity in the solar neighborhood, 2MASS 2306-0502 has been the target of extrasolar planet searches. Gillon et al. (2016) first detected three Earth-sized transiting planets, and recently Gillon et al. (2017) discovered four more transiting Earth-sized planets around this cool dwarf. With our improved parallax presented herein, we estimate that the radii of all seven planets as well as the host star would be 4% larger than previously reported.

Gillon et al. (2017) reported that the *Spitzer Space Telescope* detected two flaring events during 20 days of observation in 2016 September. We also detected one flaring event in 2009 July, which is illustrated in Figure 9. As reported in Table 3, the overall variability is 11.6 mmag in the I band, which is less than the 20 mmag limit for CTIOPI to consider a system

significantly variable. If the entire flaring event is removed, the mean variability drops to 8.2 mmag.

23 31—LP 822-101 (LTT 9580) may be a low-gravity young system based on its K I EW value and its position ~ 2 mag above the main sequence in the H-R diagram (Figure 7). However, LACEwING did not match the system to any moving group or association. Follow-up observations are necessary to confirm whether youth or multiplicity explains its overluminosity.

23 51—2MASS 2351-2537AB (LEHPM 6333) exhibits a strong perturbation on both axes in 8.3 yr of data, as shown in Figure 1(a). The photocentric orbit has not yet wrapped, implying that the orbital period is a decade or longer. Neither the CTIOPI frames nor *HST*-NICMOS images (Reid et al. 2006) resolved it. The system’s position on the H-R diagram (Figure 7) is not significantly elevated, so the secondary does not contribute much light in V , which implies a low-mass companion.

6. Summary

The astrometric, photometric, and spectroscopic observations described herein contribute to the ongoing census of the solar neighborhood. From the astrometry, we find that of 17 possible nearby systems without previous π_{trig} , 14 are within 25 pc, while three systems (LHS 2880, LP 932-83, and LP 822-101) lie between 30 and 36 pc. The selection of parallax candidates for this sample used photometric and spectroscopic distance estimates available from the literature; we find that, in all, 29 of 32 (91%) of the systems targeted are within 25 pc. In comparison, Winters et al. (2015) report a 98.5% retention rate for red dwarfs with distances estimated from accurate CCD

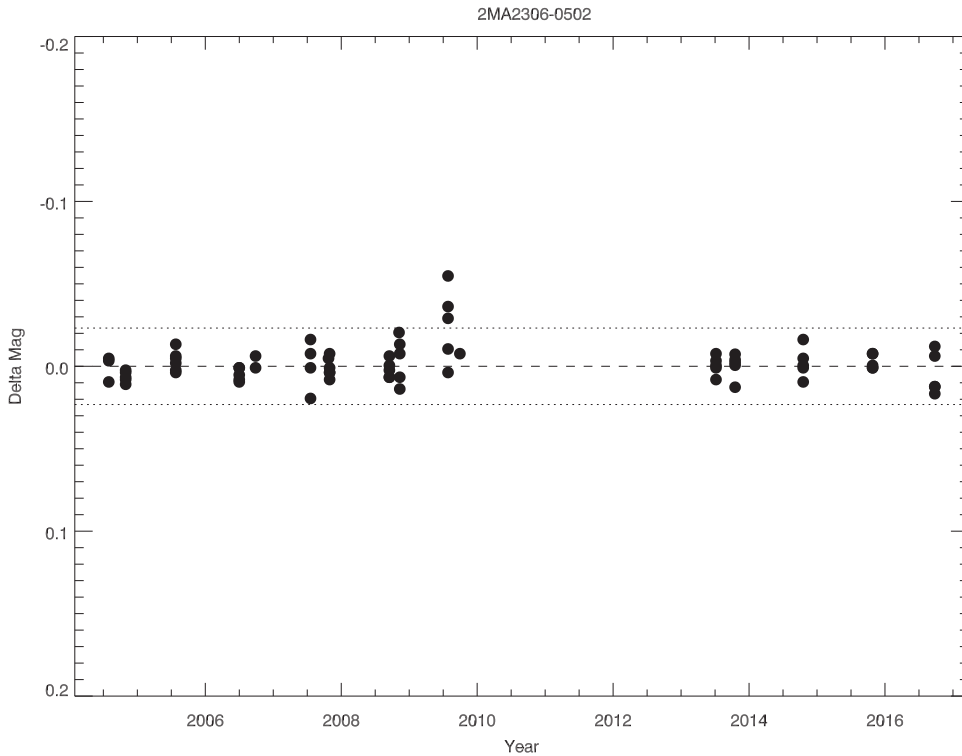


Figure 9. The light curve of 2MASS J23062928-0502285 (TRAPPIST-1) is shown around its mean instrumental magnitudes. Although it does not appear to be significantly variable, it did flare in 2009. The standard deviation of 12 mmag is calculated using 72 *I*-band images from 18 nights of observations. Based on three nights of CTIOPI photometry with the 0.9 m telescope, the *I*-band magnitude is 14.10 ± 0.03 mag.

photometry from the CTIO/SMARTS 0.9 m telescope in the systematic RECONS effort.

Because stellar proper motions are inversely proportional to distance, the nearest stars tend to display large proper motions. All but two systems in this sample have $\mu > 0''.2 \text{ yr}^{-1}$, with nine systems exceeding $0''.5 \text{ yr}^{-1}$, including 2MASS 0251-0352 and 2MASS J2306-0502 that have $\mu > 1''.0 \text{ yr}^{-1}$. Nonetheless, there are slow moving stars within 25 pc, as evidenced by 2MASS 0429-3123AB (17.0 pc) and 2MASS 1507-2000 (23.5 pc), both of which have $\mu = 0''.13 \text{ yr}^{-1}$. The resulting tangential velocities for this sample are 10.4–112.4 km s^{-1} , with a median of 27.1 km s^{-1} , which is consistent with similar populations of red dwarfs (Zapatero Osorio et al. 2007; Faherty et al. 2009; Winters et al. 2017).

Astrometry provides a means of assessing whether stars with apparently matching proper motions are physically related, via parallax and more accurate proper motion measurements. Here, we confirm that the two wide pairs LP 984-92/91 and LP 932-83/LTT 9210 are physically associated and refute that LP 731-76 is a companion to BD -10° 3166. Astrometry can also reveal unseen companions in the form of photocentric perturbations that remain once the motions for π_{trig} and μ are solved. Here, we find evidence for the companion in the previously resolved LHS 6167AB and reveal a new low-mass binary, 2MASS 2351-2537AB.

The solar neighborhood includes a smattering of pre-main-sequence stars associated with young moving groups and associations. Arguably the most important result of this work is the discovery that as many as 13 of the 32 systems targeted may be younger than ~ 120 Myr. Of these, we consider seven systems to be reliable members of β Pic, Argus, or AB Dor moving groups, whereas the remaining six should be

considered candidates. These determinations are summarized in Table 6, where details are given for three gravity indicators (Na I, Na I EW, and K I EW), H α emission levels, photometric variability, H-R diagram positions, and analyses of space motions using LACEwING and BANYAN II.

Within the solar neighborhood, the young thin disk, thick disk, and older halo components of the Galaxy are all represented to some degree. For the 15 systems in this sample with available radial velocities, *UVW* space velocities were computed for comparison with the estimated velocity dispersions of these different populations. Although several systems have motions similar to older populations, they do not lie below the main sequence in Figure 7, and we do not consider any of the systems true subdwarfs. The two L dwarfs, 2MASS 0251-0352 and 2MASS 0921-2104, which have μ greater than $0''.9 \text{ yr}^{-1}$, do lie slightly below the main sequence but in a region on this figure where the subdwarf and main sequences are not clearly separated.

For each of the systems in this sample, a homogeneous set of *VRI* photometry is now available from CTIOPI to complement the existing *JHK_s* 2MASS photometry. In addition, long-term photometric variability in the *VRI* bands reveals seven systems that vary by more than 20 mmag, the level at which we consider a star to be clearly photometrically variable. Four of these variable systems appear to have flared during the astrometric observations.

These new members of the solar neighborhood contribute to the population of coolest red dwarfs with spectral types of M3.0V to L3.0V. Through this study and the continuing CTIOPI effort, the fundamental volume-limited sample of nearby systems is becoming more complete and better understood. As the quality of the solar neighborhood census

improves, so do the physical relationships and models developed from it, yet more work remains to be done before the picture is complete.

The astrometric observations reported here began as part of the NOAO Surveys Program in 1999 and continued on the CTIO/SMARTS 0.9 m via the SMARTS Consortium starting in 2003. We gratefully acknowledge support from the National Science Foundation (NSF; grants AST 05-07711, AST 09-08402, and AST 14-12026), the National Aeronautics and Space Administration's (NASA) Space Interferometry Mission (SIM), and Georgia State University, which together have made this long-term effort possible. In addition, J.L.B. acknowledges support from the University of Virginia, Hampden-Sydney College, and the Levinson Fund of the Peninsula Community Foundation.

We thank the members of the SMARTS Consortium, who enable the operations of the small telescopes at CTIO, as well as the supporting observers at CTIO, specifically Edgardo Cosgrove, Arturo Gómez, Alberto Miranda, and Joselino Vásquez. In addition, we thank Kenneth Slatten for his meticulous review of the manuscript.

This research consulted the Set of Identifications, Measurements, and Bibliography for Astronomical Data (SIMBAD) database and the VizieR catalog access tool (Ochsenbein et al. 2000), both of which are operated at Centre de Données astronomiques de Strasbourg (CDS), Strasbourg, France. This investigation also used data products from 2MASS, which is a joint project of the University of Massachusetts and the Infrared Processing and Analysis Center (IPAC) at the California Institute of Technology funded by NASA and the NSF. In addition, this study accessed the Washington Double Star Catalog maintained at the U.S. Naval Observatory. RECONS' primary observing programs are carried out by the SMARTS Consortium, which operates four telescopes in the Chilean Andes under the auspices of the National Optical Astronomy Observatory (NOAO) and the NSF. This work used data from the European Space Agency (ESA) mission *Gaia*,²⁰ processed by the *Gaia* Data Processing and Analysis Consortium (DPAC),²¹ national institutions, in particular the institutions participating in the *Gaia* Multilateral Agreement provide funding for DPAC. Finally, computations herein employed the UVW Calculator developed by David Rodriguez.²²

Facilities: CTIO:0.9m, CTIO:1.5m.

Software: IRAF (<http://iraf.noao.edu/>), SExtractor (<http://www.astromatic.net/software/sextractor>), GaussFit (<ftp://clyde.as.utexas.edu/pub/gaussfit/>), LACEwing (<https://github.com/ariedel/lacewing>), BANYAN II (<http://www.astro.umontreal.ca/~gagne/banyanII.php>), UVW Calculator (https://github.com/dr-rodriguez/UVW_Calculator).

ORCID iDs

Jennifer L. Bartlett  <https://orcid.org/0000-0001-7394-4545>

John C. Lurie  <https://orcid.org/0000-0002-8114-0835>

Adric Riedel  <https://orcid.org/0000-0003-1645-8596>

Wei-Chun Jao  <https://orcid.org/0000-0003-0193-2187>

John P. Subasavage  <https://orcid.org/0000-0001-5912-6191>

References

- Allers, K. N., Jaffe, D. T., Luhman, K. L., et al. 2007, *ApJ*, **657**, 511
- Bartlett, J. L. 2007a, PhD diss., Univ. Virginia
- Bartlett, J. L. 2007b, *PASP*, **119**, 828
- Bartlett, J. L., Ianna, P. A., Henry, T. J., et al. 2007, *BAAS*, **39**, 772
- Bartlett, J. L., Lurie, J., Ianna, P., et al. 2016a, in AAS Meeting 227 Abstract, 142.03
- Bartlett, J. L., Lurie, J., Ianna, P., et al. 2016b, in AAS Meeting 228 Abstract, 217.03
- Bartlett, J. L., Lurie, J., Ianna, P., et al. 2017, in AAS Meeting 229 Abstract, 240.13
- Bell, C., Mamajek, E., & Naylor, T. 2016, in IAU Symp. 314, Young Stars & Planets Near the Sun, ed. J. Kastner, B. Stelzer, & S. Metchev (Cambridge: Cambridge Univ. Press), 41
- Benedict, G. F., Henry, T. J., Franz, O. G., et al. 2016, *AJ*, **152**, 141
- Bergfors, C., Brandner, W., Janson, M., et al. 2010, *A&A*, **520**, A54
- Bertin, E., & Arnouts, S. 1996, *A&AS*, **117**, 393 (SExtractor)
- Bessel, M. S. 1990, *A&AS*, **83**, 357
- Blake, C., Charbonneau, D., & White, R. 2010, *ApJ*, **723**, 684
- Boss, A., Weinberger, A. J., Anglada-Escudé, G., et al. 2009, *PASP*, **121**, 1218 (CAPSCam)
- Butler, R. P., Vogt, S. S., Marcy, G. W., et al. 2000, *ApJ*, **545**, 504
- Carpenter, J. 2006, in Explanatory Supplement to the 2MASS All Sky Data Release, ed. R. M. Cutri et al. (Pasadena, CA: IPAC), http://www.ipac.caltech.edu/2mass/releases/allsky/doc/sec6_4b.html
- Costa, E., Méndez, R. A., Jao, W.-C., et al. 2005, *AJ*, **130**, 337
- Costa, E., Méndez, R. A., Jao, W.-C., et al. 2006, *AJ*, **132**, 1234
- Cruz, K. L., Reid, I. N., Kirkpatrick, J. D., et al. 2007, *AJ*, **133**, 439
- Cruz, K. L., Reid, I. N., Liebert, J., Kirkpatrick, J. D., & Lowrance, P. J. 2003, *AJ*, **126**, 2421
- Daemgen, S., Siegler, N., Reid, I., & Close, L. 2007, *ApJ*, **654**, 558
- Davison, C. L., White, R. J., Henry, T. J., et al. 2015, *AJ*, **149**, 106
- Deacon, N., Hambly, N., & Cooke, J. 2005, *A&A*, **435**, 363
- Delfosse, X., Beuzit, J. L., Marchal, L., et al. 2004, in ASP Conf. Ser. 318, Spectroscopically and Spatially Resolving the Components of the Close Binary Stars, ed. R. W. Hilditch, H. Hensberge, & K. Pavlovski (San Francisco, CA: ASP), 166
- Delfosse, X., Forveille, T., Sègransan, D., et al. 2000, *A&A*, **364**, 217
- Deshpande, R., Martín, E., Montgomery, M., et al. 2012, *AJ*, **144**, 99
- Dieterich, S. B., Henry, T. J., Jao, W.-C., et al. 2014, *AJ*, **147**, 94
- Eggen, O. J. 1993, *AJ*, **106**, 1885
- Elias, J. H., Frogel, J. A., Matthews, K., & Neugebauer, G. 1982, *AJ*, **87**, 1029
- ESA 1997, The Hipparcos and Tycho Catalogues, ESA SP-1200 (Noordwijk: ESA), <http://adsabs.harvard.edu/abs/1997ESASP1200....E>
- Faherty, J. K., Burgasser, A. J., Cruz, K. L., et al. 2009, *AJ*, **137**, 1
- Finch, C., & Zacharias, N. 2016, *AJ*, **151**, 160
- Gagné, J., Lafrenière, D., Doyon, R., Malo, L., & Artigau, É 2014, *ApJ*, **783**, 121 (BANYAN II)
- Gaia Collaboration, Brown, A. G. A., Vallenari, A., et al. 2016a, *A&A*, **595**, A2, special *Gaia* volume (*Gaia*)
- Gaia Collaboration, Prusti, T., de Bruijne, J. H. J., et al. 2016b, *A&A*, **595**, A1, special *Gaia* volume (*Gaia*)
- Gálvez-Ortiz, M. C., Clarke, J. R. A., Pinfield, D. J., et al. 2010, *MNRAS*, **409**, 552
- Gershberg, R. E., Katsova, M. M., Lovkaya, M. N., Terebizh, A. V., & Shakhovskaya, N. I. 1999, *A&AS*, **139**, 555
- Gillon, M., Jehin, E., Lederer, S., et al. 2016, *Natur*, **533**, 221
- Gillon, M., Triaud, A., Demory, B., et al. 2017, *Natur*, **542**, 456
- Gizis, J., Monet, D., Reid, I. N., et al. 2000, *AJ*, **120**, 1085
- Graham, J. A. 1982, *PASP*, **94**, 244
- Hawley, S. L., & Petterson, B. R. 1991, *ApJ*, **378**, 725
- Henry, T. J., Jao, W.-C., Subasavage, J. P., et al. 2006, *AJ*, **132**, 2360
- Henry, T. J., & McCarthy, D. W., Jr. 1993, *AJ*, **106**, 773
- Hinkle, K., Wallace, L., & Livingston, W. 2003, in AAS Meeting 203 Abstract, 38.03
- Høg, E., Fabricius, C., Makarov, V., et al. 2000, *A&A*, **355**, L27 (Tycho-2)
- Honeycutt, R. K. 1992, *PASP*, **104**, 435
- Hosey, A., Henry, T., Jao, W.-C., et al. 2015, *AJ*, **150**, 6
- Jameson, R. F., Casewell, S. L., Bannister, N. P., et al. 2008, *MNRAS*, **384**, 1399
- Janson, M., Bergfors, C., Brandner, W., et al. 2014, *ApJ*, **789**, 102
- Jao, W.-C., Henry, T. J., Beaulieu, T. D., & Subasavage, J. P. 2008, *AJ*, **136**, 840
- Jao, W.-C., Henry, T. J., Subasavage, J. P., et al. 2003, *AJ*, **125**, 332
- Jao, W.-C., Henry, T. J., Subasavage, J. P., et al. 2005, *AJ*, **129**, 1954

²⁰ <http://www.cosmos.esa.int/gaia>

²¹ <http://www.cosmos.esa.int/web/gaia/dpac/consortium>

²² https://github.com/dr-rodriguez/UVW_Calculator

- Jao, W.-C., Henry, T. J., Subasavage, J. P., et al. 2011, *AJ*, **141**, 117
- Jao, W.-C., Henry, T. J., Subasavage, J. P., et al. 2014, *AJ*, **147**, 21
- Jefferys, W. H., Fitzpatrick, M. J., & McArthur, B. E. 1987, *CeMec*, **41**, 39 (GaussFit)
- Koen, C., Kilkenny, D., van Wyk, F., & Marang, F. 2010, *MNRAS*, **403**, 1949
- Landolt, A. U. 1992, *AJ*, **104**, 340
- Landolt, A. U. 2007, *AJ*, **133**, 2502
- Landolt, A. U. 2013, *AJ*, **146**, 131
- Lindgren, L., Lammers, U., Bastian, U., et al. 2016, *A&A*, **595**, A4, special *Gaia* volume (*Gaia*)
- Lurie, J., Henry, T., Jao, W.-C., et al. 2014, *AJ*, **148**, 91
- Luyten, W. J. 1941, in *Publications of the Astronomical Observatory, Univ. Minnesota*, Vol. 3, No. 3 (Minneapolis, MN: Univ. Minnesota Press), 33
- Luyten, W. J. 1977, in *Proper Motion Survey with the 48-inch Schmidt Telescope*, Vol. I (Minneapolis, MN: Univ. Minnesota Press)
- Luyten, W. J. 1980, *New Luyten Two-Tenths Catalogue*, Vol. 3, 4 (Minneapolis: Univ. Minnesota)
- Lyo, A.-R., Lawson, W. A., & Bessell, M. S. 2004, *MNRAS*, **355**, 363
- Malo, L., Artigau, É., Doyon, R., et al. 2014, *ApJ*, **788**, 81
- Malo, L., Doyon, R., Lafrenière, D., et al. 2013, *ApJ*, **762**, 88 (BANYAN II)
- Mamajek, E. E., Bartlett, J. L., Seifahrt, A., et al. 2013, *AJ*, **146**, 154
- Mason, B. D., Wycoff, G. L., Hartkopf, W. I., Douglass, G. G., & Worley, C. E. 2001, *AJ*, **122**, 3466
- Montagnier, G., Ségransan, D., Beuzit, J.-L., et al. 2006, *A&A*, **460**, L19
- Ochsenbein, F., Bauer, P., & Marcout, J. 2000, *A&A*, **143**, 23
- Reid, I., Cruz, K., Allen, P., et al. 2003, *AJ*, **126**, 3007
- Reid, I., Cruz, K., Kirkpatrick, J., et al. 2008, *AJ*, **136**, 1290
- Reid, I., Lewitus, E., Allen, P., et al. 2006, *AJ*, **132**, 891
- Reid, I. N., Hawley, S. L., & Gizis, J. E. 1995, *AJ*, **110**, 1838
- Reid, I. N., Kilkenny, D., & Cruz, K. L. 2002, *AJ*, **123**, 2822
- Reiners, A., & Basri, G. 2009, *ApJ*, **705**, 1416
- Riaz, B., Gizis, J. E., & Harvin, J. 2006, *AJ*, **132**, 866
- Riedel, A., Finch, C., Henry, T., et al. 2014, *AJ*, **147**, 85
- Riedel, A. R. 2016, LACEwING: LocAting Constituent mEmbers In Nearby Groups, Astrophysics Source Code Library, ascl:1601.011 (LACEwING)
- Riedel, A. R., Blunt, S. C., Lambrides, E. L., et al. 2017, *AJ*, **153**, 95 (LACEwING)
- Riedel, A. R., Subasavage, J. P., Finch, C. T., et al. 2010, *AJ*, **140**, 897
- Schlieder, J., Lépine, S., Rice, E., et al. 2012, *AJ*, **143**, 114
- Schlieder, J., Lépine, S., & Simon, M. 2010, *AJ*, **140**, 119
- Schmidt, S., Cruz, K., Bongiorno, B., Liebert, J., & Reid, I. 2007, *AJ*, **133**, 2258
- Schmidt, S. J., Hawley, S. L., West, A. A., et al. 2015, *AJ*, **149**, 158
- Scholz, R.-D., Meusinger, H., & Jahreiß, H. 2005, *A&A*, **442**, 211
- Shkolnik, E., Anglada-Escudé, G., Liu, M., et al. 2012, *ApJ*, **758**, 56
- Shkolnik, E., Liu, M., & Reid, I. 2009, *ApJ*, **699**, 649
- Siegler, N., Close, L. M., Cruz, K. L., Martín, E. L., & Reid, I. N. 2005, *ApJ*, **621**, 1023
- Skrutskie, M. F., Cutri, R. M., Stiening, R., et al. 2006, *AJ*, **131**, 1163 (2MASS)
- Slesnick, C. L., Carpenter, J. M., & Hillenbrand, L. A. 2006, *AJ*, **131**, 3016
- Song, I., Bessell, M., & Zuckerman, B. 2002, *ApJ*, **581**, L43
- Subasavage, J. P., Jao, W.-C., Henry, T. J., et al. 2009, *AJ*, **137**, 4547
- Tody, D. 1986, *Proc. SPIE*, **627**, 733 (*IRAF*)
- Tody, D. 1993, in *ASP Conf. Ser. 52, Astronomical Data Analysis Software and Systems II*, ed. R. J. Hanisch, R. J. V. Brissenden, & J. Barnes (San Francisco, CA: ASP), 173 (*IRAF*)
- Tokovinin, A., Mason, B. D., Hartkopf, W. I., Mendez, R. A., & Horch, E. P. 2015, *AJ*, **150**, 50
- Torres, C. A. O., Quast, G. R., da Silva, L., et al. 2006, *A&A*, **460**, 695
- Torres, C. A. O., Quast, G. R., Melo, C. H. F., & Sterzik, M. F. 2008, in *Handbook of Star-forming Regions, Vol. II: The Southern Sky*, ed. B. Reipurth (San Francisco, CA: ASP), 757
- Ungren, A. R., Grossenbacher, R., Penhallow, W. S., MacConnell, D. J., & Frye, R. L. 1972, *AJ*, **77**, 486
- van Leeuwen, F. 2007, *A&A*, **474**, 653
- Weinberger, A. J., Boss, A. P., Keiser, S. A., et al. 2016, *AJ*, **152**, 24
- Weis, E. W. 1994, *AJ*, **107**, 1135
- West, A. A., Hawley, S. L., Bochanski, J. J., et al. 2008, *AJ*, **135**, 785
- White, R. J., & Basri, G. 2003, *ApJ*, **582**, 1109
- Winters, J. G., Hambly, N. C., Jao, W.-C., et al. 2015, *AJ*, **149**, 5
- Winters, J. G., Henry, T. J., Jao, W.-C., et al. 2011, *AJ*, **141**, 21
- Winters, J. G., Sevrinsky, R., Jao, W.-C., et al. 2017, *AJ*, **153**, 14
- Zapatero Osorio, M. R., Martín, E. L., Béjar, V. J. S., et al. 2007, *ApJ*, **666**, 1205